

Neutrinos from Stored Muons (nuSTORM)

Submitted to the Snowmass 2021 DPF Community Planning Exercise

L. Alvarez Ruso¹, T. Alves², S. Boyd³, A. Bross⁴, P.R. Hobson⁵, P. Kyberd⁶, J.B. Lagrange⁷, K. Long^{2,7}, X.-G. Lu³, J. Pasternak^{2,7}, M. Pfaff^{2,8}, C. Rogers⁷ on behalf of the nuSTORM collaboration[†]

¹ *Instituto de Fisica Corpuscular (IFIC), Centro Mixto CSIC-UVEG, Edificio Institutos Investigación, Paterna, Apartado 22085, 46071 Valencia, Spain*

² *Physics Department, Blackett Laboratory, Imperial College London, Exhibition Road, London, SW7 2AZ, UK*

³ *Department of Physics, University of Warwick, Coventry, CV4 7AL, UK*

⁴ *Fermilab, P.O. Box 500, Batavia, IL 60510-5011, USA*

⁵ *Department of Physics and Astronomy, Queen Mary University of London, London, E1 4NS, UK*

⁶ *College of Engineering, Design and Physical Sciences, Brunel University, Uxbridge, Middlesex, UB8 3PH, UK*

⁷ *STFC, Rutherford Appleton Laboratory, Harwell Campus, Didcot, OX11 0QX*

⁸ *Department of Physics, Technical University Munich (TUM), James-Franck-Str. 1, D-85748 Garching, Germany*

Executive summary

The 2020 Update of the European Strategy for Particle Physics (ESPP) [1] recommended that muon beam R&D should be considered a high-priority future initiative and that a programme of experimentation be developed to determine the neutrino cross-sections required to extract the most physics from the DUNE and Hyper-K long-baseline experiments. The ENUBET [2–4] and nuSTORM [5, 6] collaborations have begun to work within and alongside the CERN Physics Beyond Colliders study group [7] and the international Muon Collider collaboration [8] to carry out a joint, five-year R&D programme to deliver a detailed plan for the implementation of an infrastructure in which:

- ENUBET and nuSTORM deliver the neutrino cross-section measurement programme identified in the ESPP and allow sensitive searches for physics beyond the Standard Model to be carried out; and in which
- A 6D muon ionisation cooling experiment is delivered as part of the technology development programme defined by the international Muon Collider collaboration.

This document summarises the status of development of the nuSTORM and 6D cooling experiments and identifies opportunities for collaboration in the development of the initiative outlined above.

Elements of the proposed initiative:

ENUBET

The ENUBET (Enhanced NeUtrino BEams from kaon Tagging; NP06) collaboration proposes a dedicated facility to measure ν_μ and ν_e cross-sections precisely using a combination of monitored, narrow-band neutrino beams at the GeV energy scale and by instrumenting the meson-decay tunnel with a segmented calorimeter. The ENUBET approach is based on monitoring the production of large-angle

[†]The nuSTORM collaboration is presented in the addendum.

positrons from $K^+ \rightarrow \pi^0 e^+ \nu_e$ (Ke3) decays in the decay tunnel. In addition, ENUBET will monitor muons produced in kaon and pion decays, thus providing a precise measurement of the ν_μ flux. Due to the optimisation of the focusing-and-transport system of the momentum-selected narrow-band beam of the parent mesons, the Ke3 decay represents the main source of electron neutrinos. Furthermore, the positron rate may be used to measure the ν_e flux directly. Consequently, the monitored ν_e beam will lower the uncertainties on the neutrino flux and flavour for a conventional beam from the current level of O(7%-10%) to $\sim 1\%$. Similar precision is expected for the ν_μ flux, with the bonus that the neutrino energy will be determined with a precision of $\sim 10\%$ at the single neutrino level by the “narrow-band off-axis technique”, i.e. using only the position of the ν_μ interaction vertex.

nuSTORM

The Neutrinos from Stored Muons, nuSTORM, facility has been designed to deliver a definitive neutrino-nucleus scattering programme using beams of $\vec{\nu}_e$ and $\vec{\nu}_\mu$ from the decay of muons confined within a storage ring. The facility is unique, it will be capable of storing μ^\pm beams with momentum of between 1 GeV/c and 6 GeV/c and a momentum spread of $\pm 16\%$. The neutrino beams generated will span neutrino energies from approximately 300 MeV to 5.5 GeV. This will allow neutrino-scattering measurements to be made over the kinematic range of interest to the DUNE and Hyper-K collaborations. At nuSTORM, the flavour composition of the beam and the neutrino-energy spectrum are both precisely known. The storage-ring instrumentation will allow the neutrino flux to be determined to a precision of 1% or better. By exploiting sophisticated neutrino-detector techniques such as those being developed for the near detectors of DUNE and Hyper-K, the nuSTORM facility will:

- Serve the future long- and short-baseline neutrino-oscillation programmes by providing definitive measurements of $\vec{\nu}_e A$ and $\vec{\nu}_\mu A$ scattering cross-sections with percent-level precision;
- Provide a probe that is 100% polarised and sensitive to isospin to allow incisive studies of nuclear dynamics and collective effects in nuclei;
- Deliver the capability to extend the search for light sterile neutrinos beyond the sensitivities that will be provided by the FNAL Short Baseline Neutrino (SBN) programme; and
- Create an essential test facility for the development of muon accelerators to serve as the basis of a multi-TeV lepton-antilepton collider and a Neutrino Factory.

To maximise its impact, nuSTORM should be implemented such that data-taking begins by ≈ 2030 when the DUNE and Hyper-K collaborations will each be accumulating data sets capable of determining oscillation probabilities with percent-level precision.

Muon Collider demonstrator

Muon beams of high brightness have been proposed as the source of neutrinos at a Neutrino Factory and as the means to deliver multi-TeV lepton-antilepton collisions at a Muon Collider. In most of these proposals the muon beam is derived from pion decay as is proposed here for nuSTORM. nuSTORM, which will have beams with the highest ever stored-muon beam power, will allow many of the challenges associated with the muon storage ring in such facilities to be addressed, including:

- The complete implementation of a muon storage ring of large acceptance including the injection and extraction sections; and
- The design and implementation of instrumentation by which to determine the muon-beam energy and flux to 1% or better. A novel polarimeter system will be required in order to determine the stored-muon energy and the energy spread.

The opportunity nuSTORM provides for the study of ionisation cooling is particularly important. The Muon Ionisation Cooling Experiment (MICE) [9] has demonstrated ionisation cooling in the 4-dimensional

transverse phase space [10]. To prove the feasibility of a Muon Collider therefore requires a follow-on demonstration of ionisation cooling in the full six-dimensional (6D) phase space. The facility we propose to develop will be capable of delivering the required demonstration of 6D ionisation cooling.

Opportunity:

With their existing proton-beam infrastructure, CERN and Fermilab are both uniquely well-placed to implement ENUBET, nuSTORM, and the 6D-cooling experiment as part of the required Muon Collider demonstrator. The design of ENUBET, carried out within the framework of a European Research Council funded design study, includes the precise layout of the kaon/pion focusing beamline, photon veto and timing system as well as the development and test of a positron tagger together with the required electronics and readout. The feasibility of implementing nuSTORM at CERN has been studied by the CERN Physics Beyond Colliders study group while a proposal to site nuSTORM at FNAL was developed for the last Snowmass study in 2013. The FNAL study focused on the optimisation of the muon storage ring to provide exquisite sensitivity in the search for sterile neutrinos. In the Physics Beyond Colliders study, the muon storage ring was optimised to carry out a definitive neutrino-nucleus scattering programme using stored muon beams with momentum in the range 1 GeV/c to 6 GeV/c while maintaining its sensitivity to physics beyond the Standard Model.

The study of nuSTORM is now being taken forward in the context of the demonstrator facility required by the international Muon Collider collaboration that includes the 6D muon ionisation cooling experiment. The muon-beam development activity is being carried out in close partnership with the ENUBET collaboration and the Physics Beyond Colliders Study Group. In consequence we now have the outstanding opportunity to forge an internationally collaborative activity to deliver a concrete proposal on a five-year timescale for the implementation of an infrastructure in which:

- ENUBET and nuSTORM deliver the neutrino cross-section measurement programme identified in the ESPP and allow sensitive searches for physics beyond the Standard Model to be carried out; and
- A 6D muon ionisation cooling experiment is delivered as part of the technology development programme defined by the international Muon Collider collaboration.

1 Introduction

nuSTORM, the ‘Neutrinos from Stored Muons’ facility, has been designed to provide intense neutrino beams with well-defined flavour composition and energy spectrum. By using neutrinos from the decay of muons confined within a storage ring, a beam composed of equal fluxes of electron- and muon-neutrinos can be created for which the energy spectrum can be calculated precisely. According to current design considerations, it will be possible to store muon beams with momentum from 1 GeV/c to 6 GeV/c and a momentum acceptance of $\pm 16\%$. Through its unique characteristics, the nuSTORM facility will have the capability to:

- Serve a definitive neutrino-nucleus scattering programme with uniquely well-characterised $\vec{\nu}_e$ and $\vec{\nu}_\mu$ beams;
- Allow searches for physics beyond the Standard Model and light sterile neutrinos with the exquisite sensitivity necessary to go beyond the reach of the FNAL Short Baseline Neutrino programme; and
- Provide the technology test-bed required for the development of muon beams capable of serving in a multi-TeV lepton-antilepton (muon) collider.

nuSTORM is based on a low-energy muon decay ring (see figure 1). Pions, produced in the bombardment of a target, are captured in a magnetic channel. The magnetic channel is designed to deliver a pion beam with momentum p_π and momentum spread $\sim \pm 10\% p_\pi$ to the muon decay ring. The pion beam is injected into the production straight of the decay ring. Roughly half of the pions decay as the beam passes through the production straight. At the end of the straight, the return arc selects a muon beam of momentum $p_\mu < p_\pi$ and momentum spread $\sim \pm 16\% p_\mu$ that then circulates. Undecayed pions and muons outside the momentum acceptance of the ring are directed to a beam dump. Pions from the target can also be directed to a decay channel in which low-energy muons are collected and transported to a 6D ionisation cooling experiment. ENUBET can be served with pion and kaon beams in the same complex through the addition of a third transfer line from the target complex.

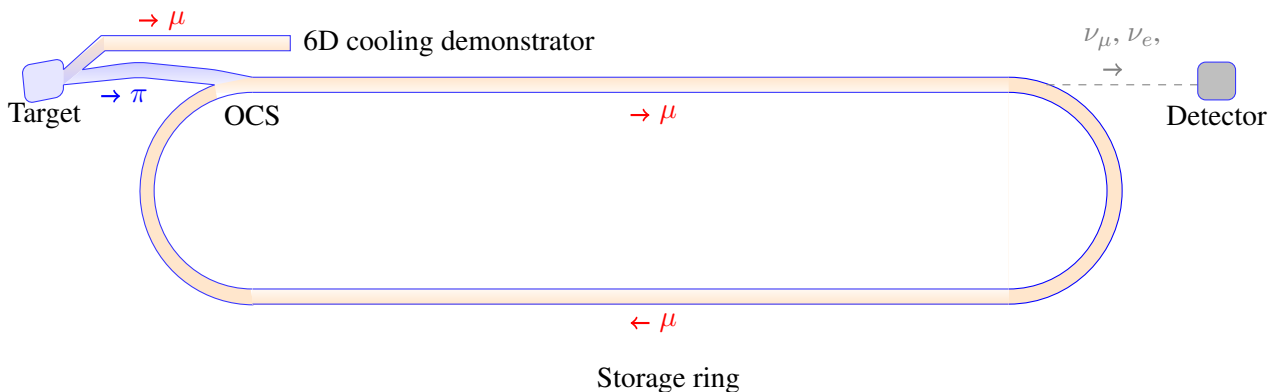


Figure 1: Schematic of the nuSTORM muon and neutrino-beam facility. The proton beam extracted from the FNAL Main Injector or the CERN SPS or PS strikes a target. Pions are collected using a horn and directed into conventional transfer lines that transport pions either to nuSTORM or a 6D muon ionisation cooling demonstration experiment. ENUBET, which requires pion and kaon beams, can be served using a third transfer line (not shown).

A detector placed on the axis of the nuSTORM production straight will receive a bright flash of muon neutrinos from pion decay followed by a series of pulses of muon and electron neutrinos from subsequent turns of the muon beam. Appropriate instrumentation in the decay ring and production straight will be capable of determining the integrated neutrino flux with a precision of $\lesssim 1\%$. The flavour composition of the neutrino beam from muon decay is known and the neutrino-energy spectrum can be calculated precisely using the Michel parameters and the optics of the muon decay ring. The pion and muon momenta (p_π and p_μ) can be

optimised to measure $\bar{\nu}_e A$ and $\bar{\nu}_\mu A$ interactions with per-cent-level precision over the neutrino-energy range $0.3 \lesssim E_\nu \lesssim 5.5$ GeV and to search for light sterile neutrinos with excellent sensitivity.

2 Motivation

The case for the nuSTORM facility rests on three themes:

1. The uniquely well-defined neutrino beam generated in muon decay can be exploited to make detailed studies of neutrino-nucleus scattering over the neutrino-energy range of interest to present and future long- and short-baseline neutrino oscillation experiments. The high-flux beams illuminating the detectors of future long-baseline experiments will allow the accumulation of very large data sets. Projections of the rate at which data will be collected in long-baseline experiments indicate that the statistical error will be reduced to the percent level by 2028–30. To optimise the discovery potential of such facilities requires that the systematic uncertainties be reduced to the percent level on a comparable timescale. This can be achieved by dedicated cross-section measurements by which to break the correlation between the cross-section and flux uncertainties and to reduce the overall systematic uncertainty to a level commensurate with the statistical and other systematic uncertainties in experiments such as Hyper-Kamiokande and DUNE.

The nuSTORM $\bar{\nu} N$ scattering programme is no less important for the next generation of short-baseline experiments for which uncertainties in the magnitude and shape of backgrounds to the sterile-neutrino searches will become critically important. At nuSTORM, the flavour composition of the neutrino beam is known and its energy spectrum may be determined precisely using the storage-ring instrumentation. The precise knowledge of the neutrino flux combined with advanced detector techniques that are currently being developed will allow nuSTORM to provide the measurements necessary to maximise the sensitivity of the next generation of long- and short-baseline experiments.

2. The nuSTORM neutrino beam instrumented with state-of-the art and magnetised near and far detectors, will allow searches for physics Beyond the Standard Model of unprecedented sensitivity to be carried out. The signal to background ratio for this combination is of order ten and is much larger than for other accelerator-based projects.
3. The storage ring itself, and the muon beam it contains, can be used to carry out the R&D programme required to implement the next step in the incremental development of muon accelerators for particle physics. Muon accelerators have been proposed as sources of intense, high-energy electron- and muon-neutrino beams at the Neutrino Factory [11, 12] and as the basis for multi-TeV l^+l^- collisions at the Muon Collider [13, 14]. An incremental approach to the development of the facility has been outlined in [15], which has the potential for the elucidation of the physics of flavour at the Neutrino Factory and to provide multi-TeV l^+l^- collisions at the Muon Collider. nuSTORM would be the first neutrino-beam facility to be based on a stored muon beam and will provide a test-bed for the development of the technologies required for a multi-TeV Muon Collider and/or a Neutrino Factory.

Just as the three legs of a tripod make it a uniquely stable platform, the three individually-compelling themes that make up the case for nuSTORM constitute a uniquely robust case for a facility that will be at once immensely productive scientifically and seminal in the creation of a new technique for particle physics.

2.1 Neutrino-nucleus scattering

nuSTORM will allow unprecedentedly precise studies of both elementary processes and neutrino-nucleus scattering to be performed. These prospects are not only interesting by themselves as a source of information about

the axial structure of nucleons and nuclei, but also crucial to achieve the high-precision goals of neutrino oscillation experiments [16, 17]. Indeed, near detectors help to reduce systematic uncertainties but do not turn oscillation analysis into a mere rescaling because near and far detectors are not identical, have different efficiencies and are illuminated by different neutrino fluxes. In addition, oscillation probabilities depend on the neutrino energy which is not known on an event-by-event basis but has to be reconstructed. To minimise any bias in neutrino-energy reconstruction a realistic simulation of the interaction process is necessary.

2.1.1 Elementary processes

In this context, by elementary processes one understands neutrino-nucleon interactions, whose relevance is often underestimated. The available information about them is scarce and comes mostly from old bubble chamber experiments. These cross-sections could be measured directly using hydrogen or deuterium targets or indirectly with the help of hydrogen-enriched targets and subtraction techniques. Examples of these are the *solid hydrogen* concept [18], where the (anti)neutrino proton interactions are obtained from the subtraction of events in plastic (CH₂) and graphite (C) targets and a high pressure TPC with hydrogen-rich gases (such as CH₄), where the cross-section on hydrogen would be extracted using *transverse kinematic imbalance* [19, 20]. nuSTORM is the ideal place for such experiments because of the precision that can be achieved. The input for event generators would be highly valuable. Furthermore, the availability of both muon and electron flavours of neutrinos under similar experimental conditions would allow the investigation of flavor-dependent features such as radiative corrections and non-standard (BSM) interactions.

The simplest elementary process is charged-current quasielastic scattering ($\nu_l n \rightarrow l^- p$ and $\bar{\nu}_l p \rightarrow l^+ n$). Even for such a basic process, which could serve as a *standard candle* to constrain neutrino fluxes, the dependence of the axial form factor (F_A) on the four-momentum transferred to the nucleon squared (Q^2) is not precisely measured. Moreover, it has been noticed recently that lattice-QCD determinations of $F_A(Q^2)$ are in fairly good agreement among themselves but in tension with empirical determinations [21] (see Fig. 2, left, taken from this review). These lattice-QCD results would imply a 20% increase of the quasielastic cross-section, as shown in the right panel of Fig. 2, also from [21].

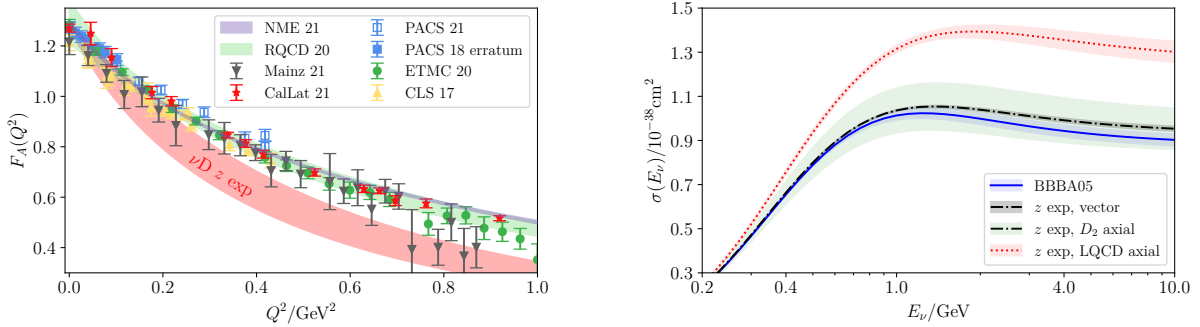


Figure 2: Left: F_A obtained in recent lattice-QCD studies compared to its determination from bubble chamber experiments using the z -expansion. Right: QE integrated cross-section from various parametrizations of the form factors. Details can be found in reference [21] from where these plots are taken.

Neutrinos also scatter inelastically on nucleons, predominantly leading to single pion (πN) but also to γN , $\pi\pi N$, ηN , ρN , KN , $\pi\Sigma$, $\bar{K}N$, KY , ... final states. For inelastic processes, the cross-section arises from the interplay of resonant and non-resonant amplitudes, which become highly non-trivial at higher invariant

mass hadronic final states, with several overlapping resonances and coupled channels. This is the shallow inelastic scattering region, where a large fraction of events at DUNE will be found. The dynamics have been investigated in detail in partial wave analyses of large data sets available for photon, electron and pion-nucleon interactions. This information is valuable to constrain weak inelastic processes and has been used in their modelling as reviews, for instance, in reference [22]. However, the properties of the axial current at finite Q^2 remain experimentally unconstrained. The transition from the resonant to the deep-inelastic scattering regime is also highly uncertain. Quark-hadron duality on one hand and QCD (higher-twist and target mass) corrections on the other are valuable tools to describe it (see reference [23] for a recent review), but progress in their development is hindered by the lack of experimental nuclear-effect-free information from elementary targets. With muon momenta in the range $1 \leq p_\mu \leq 6 \text{ GeV}/c$, the resulting neutrino spectrum goes up to $\sim 5.5 \text{ GeV}$ and would make the detailed study of this region possible.

2.1.2 Neutrino-nucleus interactions

There is considerable interest in the study of neutrino scattering on the heavy targets used in oscillation experiments. nuSTORM will have a strong impact by characterising the flavour differences which are particularly important at low energy and momentum transfers (in the laboratory frame). These differences can arise from a subtle interplay between lepton kinematic factors and response functions [24]. The search for CP-invariance violation in present and planned long-baseline neutrino-oscillation experiments is based on the measurement of the rate of ν_e appearance in ν_μ beams. nuSTORM has the potential to perform high-statistics measurements of the $\overline{\nu}_e$ cross-sections and, in particular, the $\sigma(\nu_e)/\sigma(\nu_\mu)$ cross-section ratio, which is among the largest systematic uncertainties at DUNE [25]. With the help of nuSTORM, the required sensitivity to CP violation can be reached with a smaller exposure.

Measurements of quasielastic-like scattering at nuSTORM can also lead to a better description of initial state nucleon-nucleon correlations and meson-exchange currents, which are known to provide a sizeable contribution to the semi-inclusive electron scattering cross-section and have been found important at MiniBooNE and T2K: comparisons of different theoretical results to data can be found, for example, in Figures 8-9 of reference [26] (MiniBooNE) and in Figures 7-9 of reference [27] (T2K). The comparisons of the SUSA model to these data have been recently summarised in reference [28]. Discrepancies with theory (or, at least with its generator implementation) have been found at the higher energy and momentum transfers probed at MINERvA and NOvA as can be appreciated in references [29, 30]. With unprecedented understanding of the beam flux (see section 3.3) and sophisticated detector designs (see section 3.2), nuSTORM can play an important role in understanding these differences.

The characterisation of nuclear corrections to parton distribution functions will also benefit from precise measurements of the inclusive neutrino-nucleus cross-section, to unravel the differences in nuclear effects observed in weak and electromagnetic processes and to resolve the tensions that have been observed by nCTEQ. It was suggested that νA and $l^\pm A$ data could only be reconciled if the correlations in νA were not taken into account. However, a more recent comprehensive nCTEQ analysis indicates that neglecting correlations does not relieve the tension between νA and $l^\pm A$ data. More precise data on a wider variety of nuclear targets would be most welcome.

With a suitable detector set, nuSTORM can also study exclusive channels in neutrino-nucleus scattering (see section 3.4). These include one and two-nucleon knockout but also single and multiple meson production. These reactions are largely influenced by strong final state interactions between the produced particles and the nuclear environment. Pions, in particular, can scatter, change charge or be absorbed on their way out of the nucleus [31]. Pion production will play an important role in the future neutrino oscillation programme. Pioneering measurements of pion production by MINERvA (cf. review article [32] and references therein) have

shown tensions with model predictions (see, for example, figure 3). Accurate modelling of these interactions are crucial to reduce biases in calorimetric neutrino energy determination.

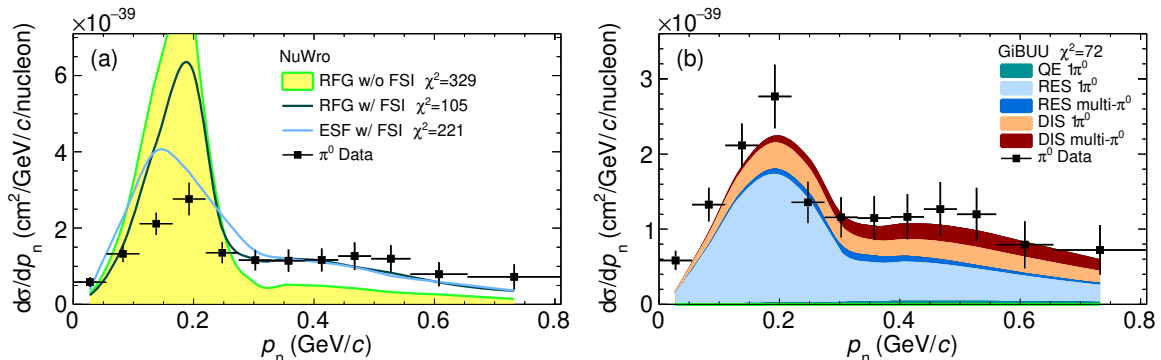


Figure 3: Flux-averaged differential cross-section in the emulated nucleon momentum, p_n , measured by MINERvA with the Low-Energy NuMI beam flux peaking at 3 GeV on a scintillator (CH) target. The peak region of the p_n distribution directly reflects the Fermi motion of the struck neutron in the charged-current π^0 production [33–35]. Comparisons with NuWro [36] and GiBUU [37–39] predictions are made. Figures from reference [40].

2.2 Searches for physics beyond the Standard Model

2.2.1 Rare scattering processes

If the precision of the nuSTORM concept is combined with high statistics, the study of *rare* processes with small cross-sections becomes feasible. Processes in this category include neutrino-electron scattering, coherent meson production, weak and electromagnetic production of single photons and dileptons. In addition to elementary quasielastic scattering, neutrino-electron scattering or even coherent meson production could be precisely measured and used as *standard candles* for flux determination in other experiments. Furthermore, weak couplings and $\sin^2 \theta_W$ can be extracted, providing a precision test of the Standard Model (SM). Unlike DUNE, nuSTORM has access to both ν_μ – and ν_e –electron scattering.

While these exotic processes are allowed in the SM, precision measurements can disclose physics beyond the Standard Model (BSM). This is the case in neutrino tridents in which neutrino scattering off the Coulomb field of a heavy nucleus generates a pair of charged leptons. The existence of light Z' or other particles in the dark sector can modify the trident cross-section [41].

Single photon emission in neutral current interactions is another rare process that has received attention as a background in ν_e appearance measurements in Cherenkov detectors. Its cross-section has never been measured and, so far, only upper limits from NOMAD, T2K and, more recently, MicroBooNE are available. Besides, some of the proposed explanations of the MiniBooNE anomaly involve the production of a heavy (1–100 MeV) neutrino via electromagnetic (γ mediator), weak (Z) or BSM (Z') interactions, leading to a signal in the single photon or e^+e^- channels (see reference [42] for a recent review). While recent MicroBooNE results disfavour some explanations of the MiniBooNE anomaly, the full range of possible solutions is still unexplored [43].

2.2.2 Short-baseline flavour transitions and sterile neutrino searches

The unique neutrino beam composition at nuSTORM allows to use $\mu^+ \rightarrow e^+ \nu_e \bar{\nu}_\mu$ decay to search for short-baseline oscillations using muon final states. In particular, for the first time, nuSTORM would allow to search for ν_μ appearance from $\nu_e \rightarrow \nu_\mu$ oscillations, which is not subject to photon-like and intrinsic ν_e contamination as in other accelerator experiments. This appearance measurement relies on a good charge identification to discriminate the μ^- signal from the intrinsic μ^+ background from the muon-decay $\bar{\nu}_\mu$ component. The latter can also be used to search for $\bar{\nu}_\mu \rightarrow \bar{\nu}_\mu$ disappearance. The low flux systematics allow to reach greater levels of precision in the total normalisation of the event rate, and one can expect this measurement to be limited by the cross-section uncertainties. Nevertheless, greater sensitivity can be achieved by identifying spectral distortions of the μ^+ spectrum in the detector; this would require accurate momentum measurement.

In Ref. [44], a detailed study of the sensitivity of the previous Fermilab design of nuSTORM to sterile neutrinos was performed. This was based on a far detector located at 2 km from the muon storage ring and a total of 10^{21} POT, corresponding to approximately 2×10^{18} useful muon decays. The detector was a 1.3 kt magnetised iron-scintillator detector with excellent muon charge discrimination. The final sensitivity was found to be greater than 5σ throughout the entire region of oscillation parameter space preferred by the MiniBooNE and LSND results. Ref. [6] expanded the scope of the oscillation search to show that nuSTORM can also provide very stringent tests of the unitarity of the neutrino mixing matrix, non-standard interactions, as well as Lorentz and CPT symmetries.

In summary, nuSTORM would be capable of addressing open questions concerning the non-unitarity of the neutrino mixing matrix, non-standard interactions, Lorentz invariance (and CPT violation) and provide a definitive test of light sterile neutrinos [6, 44].

2.3 Technology test-bed

A Muon Collider has the potential to deliver lepton-anti-lepton collisions at centre-of-mass energies up to 10 TeV at a cost and on a timescale advantageous when compared to electron-positron or next-generation hadron colliders [45]. The international Muon Collider collaboration is developing conceptual designs for facilities capable of operation at centre-of-mass energies of 3 TeV and 10 TeV [8].

nuSTORM will have the world's highest power stored muon beam. Such a beam will provide the opportunity to develop and test technologies that will be critical to the delivery of muon beams with the brightness necessary for the Muon Collider to deliver the specified luminosity of $\sim 10 \times 10^{34} \text{ cm}^{-2} \text{ s}^{-1}$. In particular, a low-energy muon beam may be produced through the capture of an appropriate pion-beam phase space at the nuSTORM target. The muon beam derived from pion decay could be directed towards a muon ionisation cooling system designed to demonstrate the feasibility of reducing the muon-beam phase space in all six phase-space dimensions.

The principle of ionisation cooling was demonstrated by the MICE collaboration [10]. The MICE experiment determined the change in the transverse emittance of a muon beam as it passed through a single liquid-hydrogen or lithium-hydride absorber. The muon beams used by MICE had momentum in the range 140 MeV/c to 240 MeV/c and emittance in the range 3 mm to 10 mm. For the Muon Collider to achieve its design luminosity requires transverse and longitudinal emittances of $25 \mu\text{m}$ and 7.5 MeV m respectively. An experiment based on the lessons learnt at MICE, can be used to develop the techniques to compress the 6D phase-space volume of a muon beam to the values required to achieve the luminosity specification of the Muon Collider.

2.3.1 Muon ionisation cooling

Ionisation cooling is effected by passing a muon beam through a material (the absorber), in which it loses energy, and subsequently accelerating the beam to restore the energy lost in the absorber. The ionisation cooling process occurs on a short timescale and is therefore able to cool the beam efficiently with modest decay losses. The net effect of the energy-loss/re-acceleration process is to reduce the transverse beam size, i.e. to reduce the *transverse emittance*.

Multiple Coulomb scattering is detrimental to the cooling performance. Energy absorbers made from materials having low atomic number, such as lithium or hydrogen, are preferred as the ratio of ionisation energy loss to multiple Coulomb scattering is favourable. If the beam is tightly focused the effect of multiple Coulomb scattering relative to the intrinsic beam divergence is reduced. Therefore ionisation cooling lattices must be designed to maintain very tight focusing.

Random fluctuations in energy loss, known as energy straggling, tend to result in an increase in the beam-energy spread and hence longitudinal emittance. It is possible to reduce the longitudinal emittance of the beam by introducing a dipole and wedge-shaped absorber onto the beamline. The dipole bends lower momentum particles more strongly, introducing a correlation between energy and position. By aligning the thicker part of the wedge with high energy particles and the thinner part of the wedge with low energy particles, the energy spread is removed and replaced with an increased spread in position. This is an emittance exchange process; the energy spread of the beam is decreased at the expense of an increased transverse emittance. Transverse emittance, in turn, is reduced by the ionisation cooling process. Overall the size of the beam in the 6D phase space (x, p_x, y, p_y, t, E) is reduced.

2.3.2 6D cooling system design

The baseline design for the Muon Collider ionisation cooling system is of order 1 km long. The main part comprises the rectilinear cooling system described in [46]. In this system, focusing is achieved by means of solenoids having fields up to around 12 T. A weak dipole field is introduced that creates a position-energy correlation and wedge-shaped absorbers are used to deliver 6D cooling. Early parts of the system, where the beam has large emittance, are optimised for large acceptance, while later parts of the system are optimised for cooling to low emittance.

The proposed demonstrator facility would comprise around 50 m of cooling equipment, as shown in figure 4. Low momentum pions are diverted from the target region by means of a dipole switchyard. Off-momentum pions are rejected and the resultant beam is collimated while the pions decay to muons. Collimation is necessary in order to deliver a low emittance beam suitable for demonstration of later stages of the cooling system. A short, high voltage section of RF then accelerates or decelerates particles that are out of phase with the RF cavities yielding a bunched beam. Finally, a short focusing system is used to ensure parameters such as muon-beam divergence and position spread are matched to the cooling channel focusing system.

For beam cooling, a tightly packed lattice of RF cavities, absorbers and solenoids is envisaged. The later stages of the rectilinear cooling system operate in the second stability region, where each cell of the magnet lattice has two foci; one at the absorber and a weaker focus in the centre of the RF cavities. This can be achieved with solenoids having fields up to about 10 T. Sufficient dispersion can be achieved by appropriate choice of dipole polarity and field, so that low angle wedges can be used while yielding a satisfactory longitudinal cooling performance.

Instrumentation is required upstream and downstream of the cooling system to measure the beam emittance and a dedicated section of beamline is foreseen to support this. Additional instrumentation is required in each module to support operations such as beam alignment and RF phasing. Beam intersecting devices or instru-

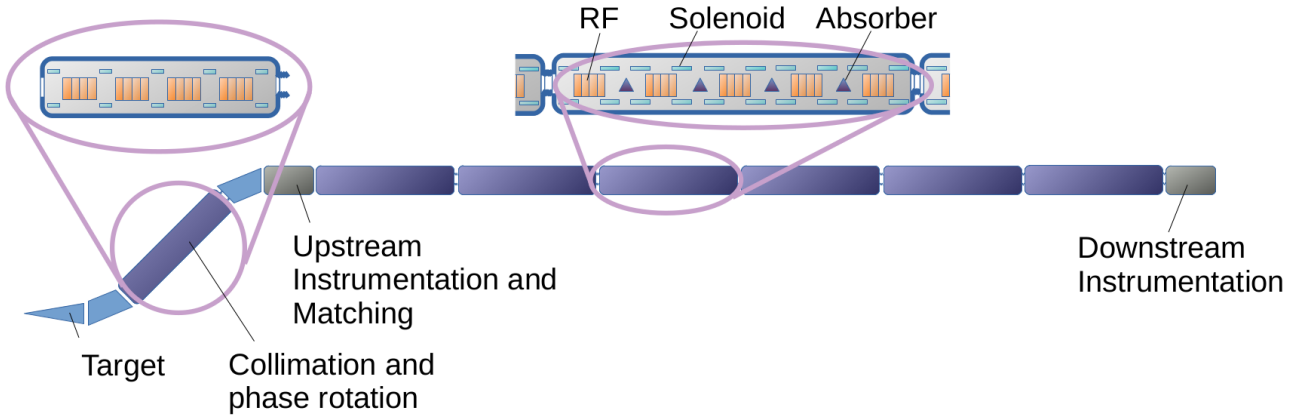


Figure 4: Schematic of a possible implementation of the Muon Collider demonstrator for 6D cooling.

mentation of the absorbers may be an effective means of monitoring the muon beam, less readily achievable in a more conventional beamline.

3 nuSTORM facility; overview

The following sections give a brief description of the development of the nuSTORM concept since it was presented in [6]. The authors are actively developing the accelerator design, the detector concept, and the analysis framework. Therefore the summary presented below should be considered a snapshot in the development of the nuSTORM facility.

3.1 Accelerator facility

3.1.1 Target and pion transport

The feasibility of implementing nuSTORM at the SPS at CERN was presented in [6]. The proton beam extracted from the SPS at 100 GeV is focused on a solid (low- Z) target placed inside a focusing horn. In the simulations presented below, the proton beam impinges on an inconel target. Other materials for the target, such as graphite, may be considered. Particles emerging from the target are focused by the horn and collected in a short transfer line with a large momentum acceptance of $\sim \pm 10\%$. The transfer line is composed of dipoles, collimators and quadrupoles. It is proposed that the target, horn and the initial part of the transfer line are contained in an inert helium atmosphere to reduce activation and corrosion of beam-line equipment by limiting the presence of ozone and nitrogen oxides. The target-and-collection system will be installed underground in a cavern, with a shaft giving access to a surface building. The shaft and surface buildings will be offset with respect to the incoming proton beam direction, the target, and the outgoing pion beam.

The design of the pion transfer line is based on the initial FNAL design. The design was modified to accommodate the projected radiation hazards and an improved injection scheme. A modular construction scheme, allowing for a greater degree of flexibility during the design phase and using simple quadrupole FODO cells and achromatic dipole bends, was adopted. An initial capture section will be present inside the initial containment vessel, which will be followed by the proton absorber. A series of collimators will be used in addition to the bending sections to reduce the radiation load on the downstream beam lines.

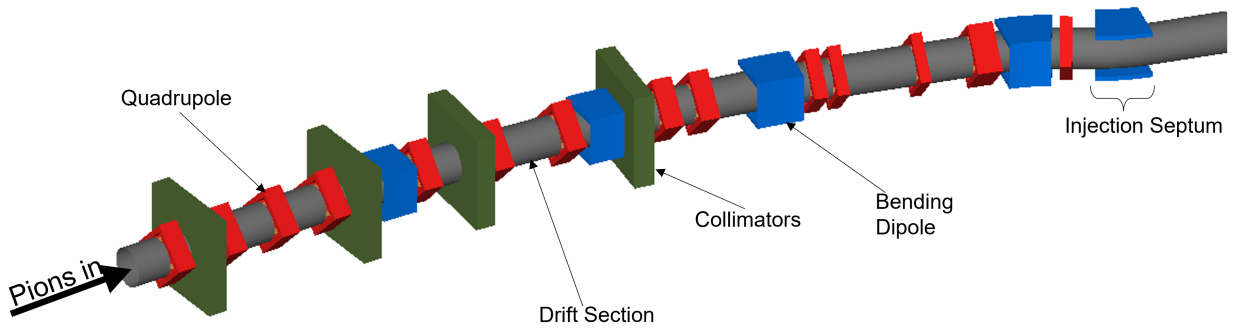


Figure 5: Schematic drawing of the pion transfer line generated in BDSIM code.

The first achromatic bending section is used to divert particles within the desired momentum range away from the proton absorber towards the ring. This is key to reduce the radiation dose to downstream elements and provide a momentum selection for the transmitted pion beam. A quadrupole FODO lattice is used to transport the beam to a second achromatic bending section followed by beta-function matching and injection into the ring. The length of this section was chosen to ensure the radiation contamination within the arc sections of the ring is minimised, whilst being short enough to ensure that pions of low momentum can be successfully transported. Building on [6], the beta-function and dispersion matching section has been defined and the first integration of the transfer line with the ring injection system has been performed.

Pion production in the target was simulated using MARS [47] and FLUKA [48, 49]. The particle-distribution was used as input for beam-dynamics studies of the transfer line using BDSIM code [50]. The beam dynamics simulations confirmed the large momentum acceptance of the transfer line. The layout of the transfer line simulated in BDSIM is shown in figure 5. The optical functions of the transfer line, shown in figure 6, were reproduced using beam dynamics simulations in BDSIM. The values of the optical functions obtained with BDSIM agree well with the design values and provide the correct beam conditions at the injection to the ring.

3.1.2 Storage ring design

The nuSTORM decay ring, shown schematically in figure 7, is a compact racetrack storage ring with a circumference of ~ 616 m that incorporates large aperture magnets. In order to include the orbit combination section (OCS), used for the stochastic injection of the pion beam into the ring, a dispersion suppressor is needed between the arc and the production straight. Strong bending magnets are also needed in the arcs to minimise the arc length, in order to maximise the number of useful muon decays.

Several designs for the nuSTORM storage ring have already been proposed based either on a separated function magnet or Fixed Field Alternating gradient (FFA) approach [51–53]. To serve the neutrino-scattering programme, the ring was redesigned to store muon beams with a momentum of between 1 GeV/c and 6 GeV/c with a momentum acceptance of up to $\pm 16\%$, thereby increasing the neutrino flux. To keep the momentum acceptance and transverse dynamic acceptance large, and simultaneously to maximise the muon accumulation efficiency, a hybrid concept was developed (figure 7). Conventional FODO optics, used in the production straight, are combined with FFA cells, for which the chromaticity is zero, in the arcs and in the return straight. This allows the revised lattice to achieve:

- Zero dispersion in the quadrupole injection/production straight;
- Zero chromaticity in the arcs and in the return straight, thereby limiting the overall chromaticity of the ring; and thus
- Large overall transverse and momentum acceptance.

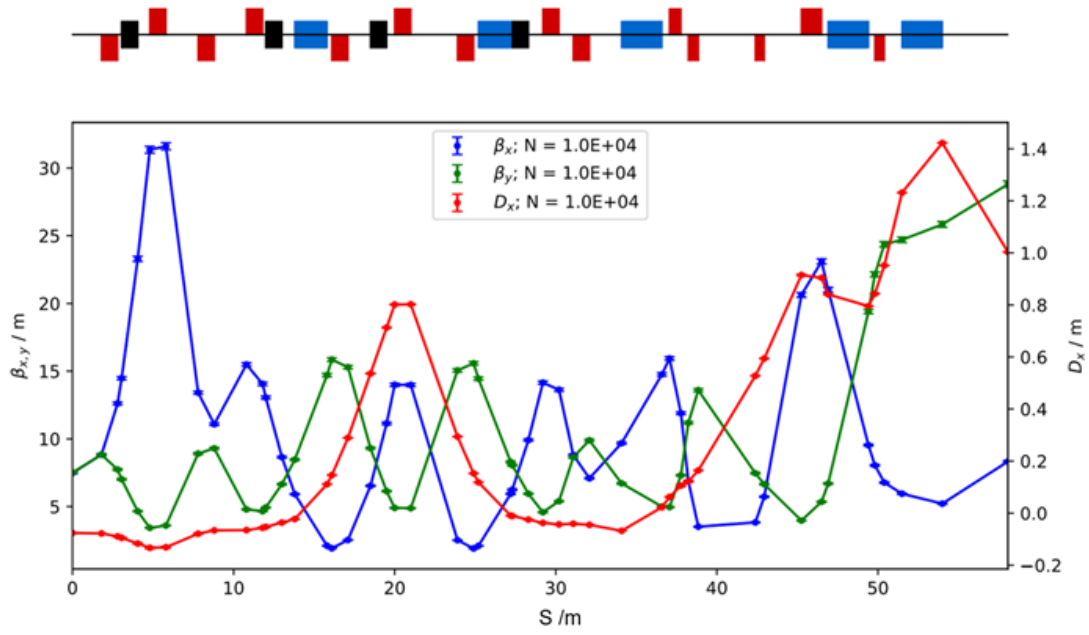


Figure 6: The β functions (β_x - blue, β_y - green) and dispersion (D_x - red) in the pion transfer line downstream from the horn until the end of the injection septum generated using beam dynamics simulations in BDSIM code.

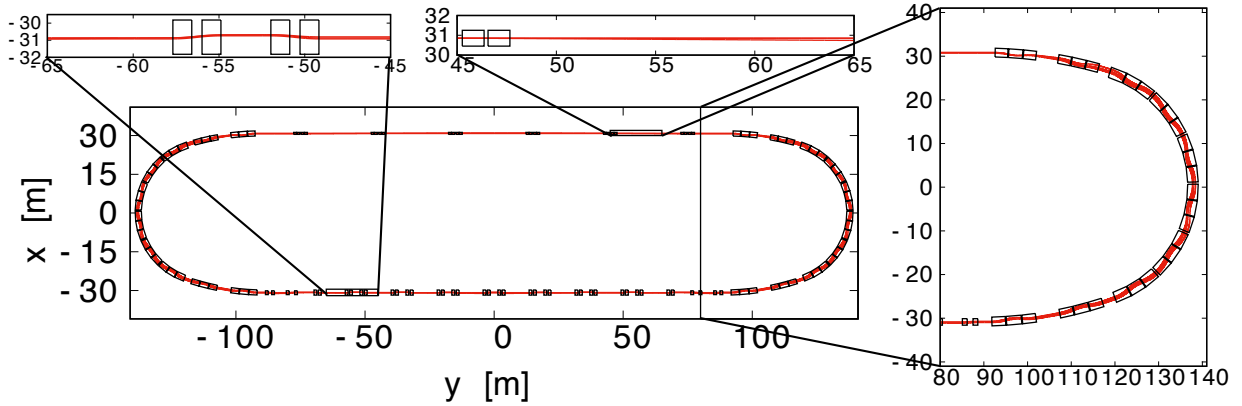


Figure 7: Schematic drawing of the revision of the muon storage ring. The beam circulates in an clockwise direction. The production straight (at $x \sim 30$ m) is composed of large aperture quadrupoles that produce the large values of the betatron function required to minimise the divergence of the neutrino beam produced in muon decay. The lattices of the arcs and return straight are based on the Fixed Field Alternating gradient (FFA) concept and allow a large dynamic aperture to be maintained.

The arcs exploit superconducting combined-function magnets with magnetic fields of up to ~ 2.6 T. The return straight is based on combined-function room-temperature magnets. The production straight uses large-aperture room temperature quadrupoles. The vertical magnetic field around the ring for the maximum momentum (~ 6 GeV/c) muon closed orbit in the racetrack FFA ring is shown in figure 8. The mean betatron functions in both the production and return straights are kept large enough to minimise the contribution of betatron oscillations to the angular spread of the neutrino beam, such that both can be used to serve a neutrino-physics programme.

The arc cells have a high magnet-packing factor to minimise the arc length and are connected with the injection and return straights using specific matching sections. The matching section serving the injection straight matches dispersion to zero and allows a long straight for injection to be accommodated. Additional matching sections are between the arcs and the cells of the return straight. The Twiss parameters around the ring are shown in figure 9. Selected parameters of the hybrid design for the racetrack ring are summarised in table 1. The reference tunes of the machine (8.203, 5.159) are chosen such that they are not close to the dangerous resonances. The off-momentum tunes have been chosen to avoid integer and half-integer resonances (see figure 10). Further reduction of the chromaticity of the ring is possible by altering the nonlinear magnetic field distribution in the regular arc cells.

Total circumference	616 m
Length of one straight section	180 m
One straight section/circumference ratio	29%
Operational momentum range	1–6 GeV/c
Reference momentum	5.2 GeV/c
Reference tunes (Q_h, Q_V)	(8.203, 5.159)
Momentum acceptance	$\pm 16\%$
Number of cells in the ring:	
Straight quad cells	6
Arc first matching cells	4
Arc cells	12
Arc second matching cells	4
Straight matching FFA cells	1 (+1 mirror)
Straight FFA cells	8

Table 1: Selected parameters of the hybrid FFA storage ring.

The performance of the hybrid FFA design for the storage ring was verified in tracking studies. In order to incorporate tracking through the combined-function magnets, taking into account the fringe fields and large amplitude effects, a code used for the full FFA machine developed previously was used [53]. It is a stepwise tracking code based on Runge-Kutta integration, using Enge-type fringe fields. The results of the multi-turn tracking show that the dynamical acceptance of the machine is about 1π mm rad in both transverse planes, which is required for the needs of the experimental programme, as shown in figure 11. The studies to cross-check the results with the PyZgoubi code, as performed successfully before [53], are underway.

3.2 Detector considerations

As has been described, the detector at the nuSTORM facility will deliver a rich programme of neutrino-interaction physics that can be explored with unprecedented precision and an unprecedented reach in searches for new phenomena. In order to take full advantage of these opportunities, the detector requirements extend far

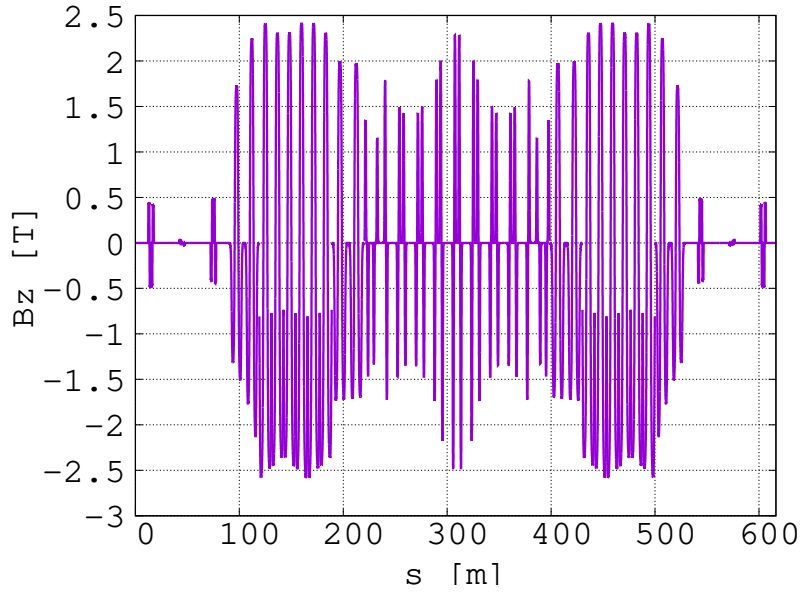


Figure 8: The vertical magnetic field for the maximum momentum ($\sim 6 \text{ GeV/c}$) muon closed orbit in the racetrack FFA ring.

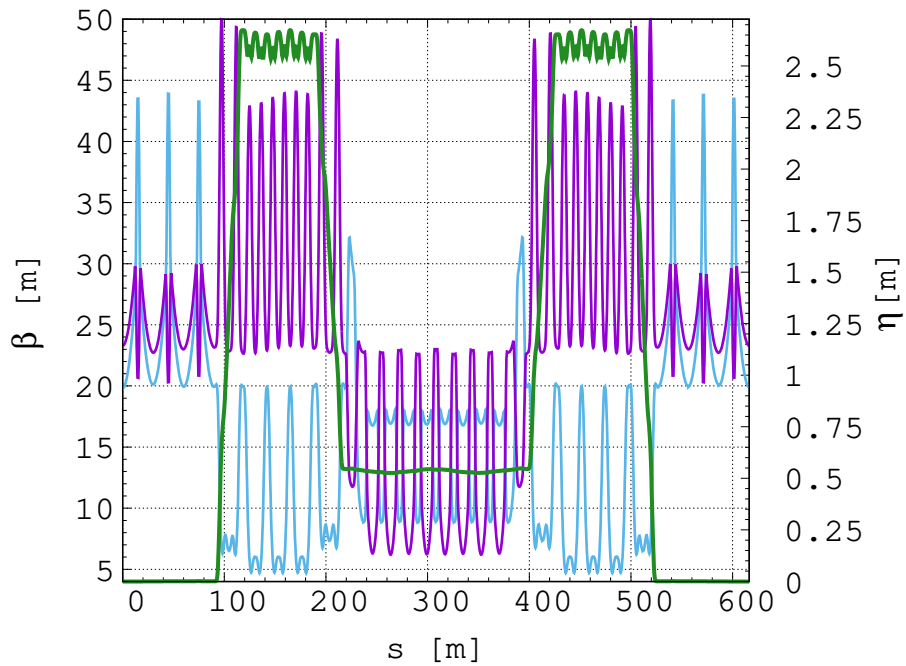


Figure 9: The betatron functions (horizontal-blue and vertical-purple) and dispersion (green) for reference momentum (5.2 GeV/c) muon closed orbit in the racetrack FFA ring.

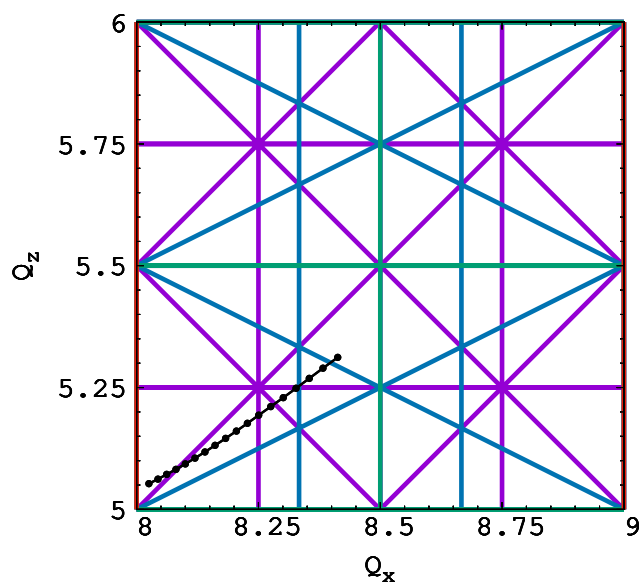


Figure 10: The machine tunes for the muon beam stored in the nuSTORM ring at the reference momentum of 5.2 GeV/c with the momentum spread of $\pm 16\%$.

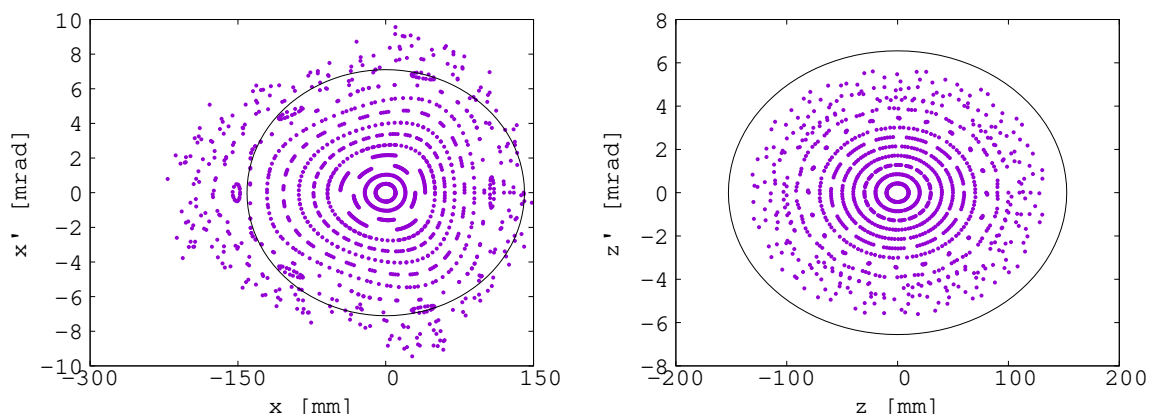


Figure 11: The horizontal (left-hand plot) and the vertical (right-hand plot) dynamical acceptance studies in the hybrid nuSTORM ring at the reference momentum of 5.2 GeV/c. Particles are tracked over 100 turns with different amplitudes in the plane of study including a small off-set from the closed orbit in the other plane. The black ellipse represents the acceptance of 1π mm rad.

beyond that needed for a 3-flavor oscillation search. Options for the detectors are discussed below, but we list some of the overarching performance requirements here:

- Highly segmented detectors capable of operation at high event rate. Detectors with precise 3D tracking (or very precise timing) capability over 4π are required.
- Detectors with excellent muon and electron ID capability.
- Detectors with excellent energy resolution.
- A magnetised detector so that the charge of the muon and electron in the final state can be determined. In addition reconstruction via spectrometry can be applied to event reconstruction as opposed to being done via calorimetry. This is particularly important for higher energy nuSTORM tunes neutrino interactions where the outgoing muon's momentum must be measured via spectrometry.
- Detectors with excellent hadronic particle ID, i.e. $p/\pi/K$ separation at momenta from a few hundred MeV/c to a few GeV/c.
- Detectors with neutron detection capability (with energy determination).
- A detector that presents a variety of nuclear targets to measure cross-sections as a function of the nuclear target mass number A .

Many of the detector concepts now incorporated in the upgraded T2K near detector [54] and those being developed for DUNE [55] are appropriate for detectors at nuSTORM. These concepts include:

1. Highly-segmented tracking scintillator detector (SuperFGD);
2. Pixelated LAr detector;
3. Magnetised high-pressure gaseous Ar TPC (HPgTPC);
4. Straw-Tube trackers (STT) with thin targets.

Magnetisation of all these detectors is under consideration. The SuperFGD for T2K is a magnetised detector as will be the STT for DUNE. The HPgTPC is by design a magnetised detector. Although magnetisation concepts for a pixelated LAr have been developed, the high cost for the magnet system presents obstacles to its use, although R&D on high-temperature superconductor and cable may make this option affordable.

Although the concept of magnetisation in neutrino detectors is not new, the application of a collider-detector design for neutrino physics is. One such example is the high-pressure gas TPC (HPgTPC) detector concept (called ND-GAr) for the DUNE near detector complex [56]. An overview of the detector is shown in Figure 3.2. ND-GAr is a large detector with a magnetic volume that is approximately 7 m in diameter and 7.5 m long (both the HPgTPC and the ECAL are in the magnetic volume). The solenoid magnet and the return iron provide pressure containment. This detector offers many advantages including: capability to vary the target nucleus (main gas component) from He to Xe, operation at pressures from 1 Bar to 10 Bar, 4π tracking with track thresholds down to 5 MeV, excellent particle ID which allows for very precise determination of exclusive final states and the addition of a magnetic field allows for energy measurement via spectrometry as well as calorimetry (from the ECAL). In DUNE, ND-GAr functions as muon catcher for the pixelated LAr detector which is just upstream. The return iron has a window which allows muons that exit the LAr to be accurately momentum analysed in the HPgTPC.

3.3 Neutrino fluxes

We consider the neutrino energy spectrum at the front face of a detector of area 5 m by 5 m placed 50 m beyond the end of the nuSTORM production straight. We present the results for two pion energies, 3 GeV and 5 GeV and three neutrino signals: ν_μ from pion decay in the production straight, referred to as pion flash; ν_μ and ν_e from muon decays in time with the pion decays in the production straight; ν_μ and ν_e from muons which decay in the production straight of the nuSTORM ring after the end of the pion flash. These numbers for the 5 GeV pion beam are normalised to the number of protons on target; for the 3 GeV beam there are still unexplained

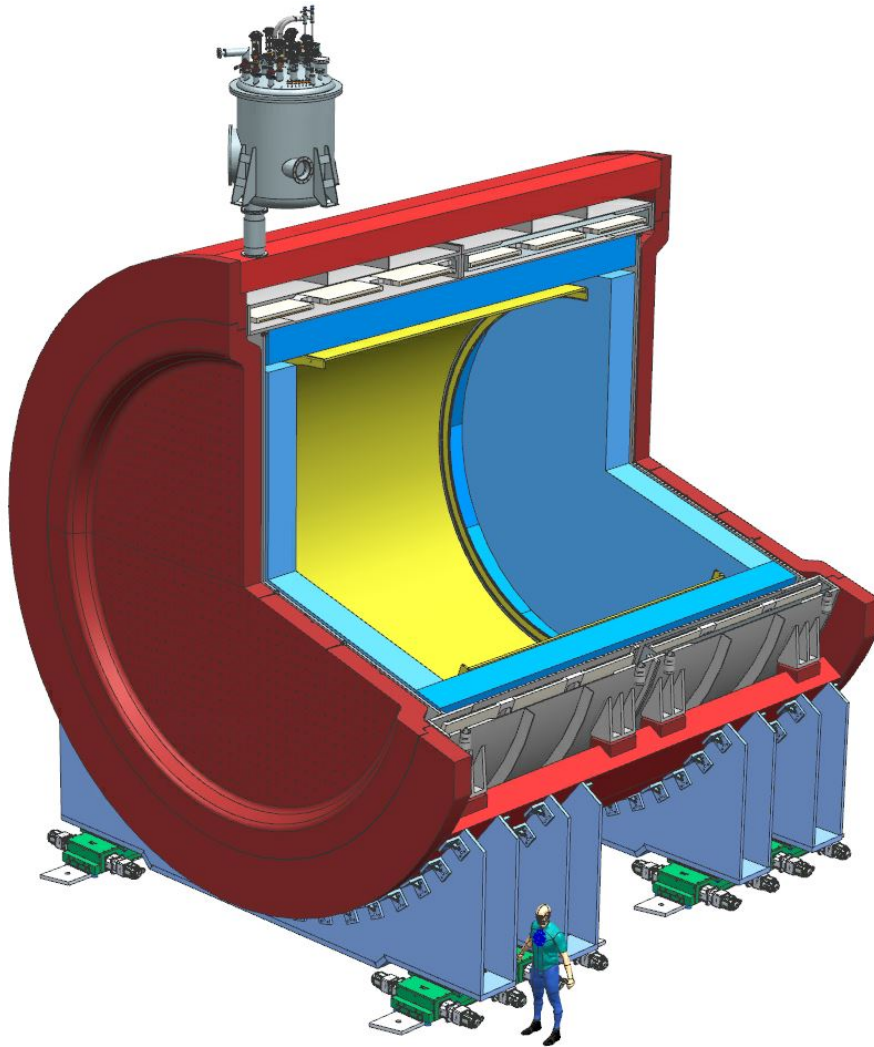


Figure 12: Schematic of the ND-GAr concept. From inside out, Yellow: HPgTPC, Blue: ECAL, Grey: Superconducting solenoid in its cryostat and Red: Return Iron.

losses in the FLUKA simulation and so we show results normalised to the number of pions accepted by the transfer line. The number of pions produced when modelling the production target with MARS and FLUKA are sufficiently different that attempting to normalise rates to protons on target would be misleading. The results are presented assuming a 100 GeV proton beam on the production target; we have not considered in detail the effect of using the 26 GeV beam from the CERN PS. The distributions are similar in pion angle and energy, but the 100 GeV beam produces about a factor of 5 more pions at all energies. At present we are agnostic on the choice of primary beam energy, merely noting that a lower energy requires more intensity or longer running for the same sensitivity.

Neutrinos from muons which decay before they reach the end of the production straight and are captured by the ring, overlap in time with the pion decays in the production straight and constitute a background to the pion flash signal of around 1%. While neutrinos from muons which are captured by the nuSTORM ring and decay during subsequent rotations round the ring, are essentially background free. A number of other sources of backgrounds are considered and where it can be shown that the contamination will be well below 1%, no attempt is made to simulate them in detail. A description of the simulation and background estimation can be found in Appendix A and B.

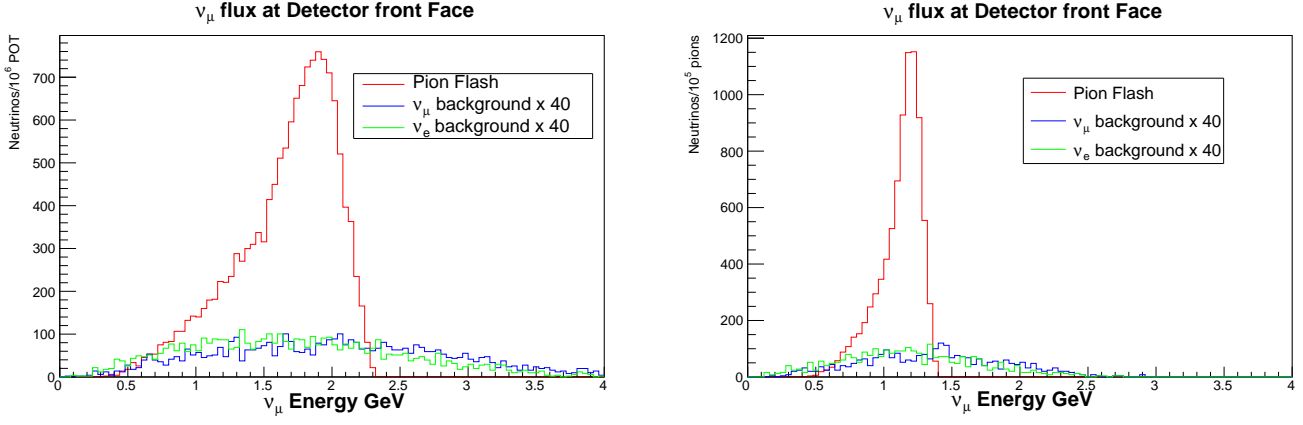


Figure 13: Left: Pion flash energy spectrum for $E_\pi=5$ GeV and associated muon backgrounds. Right: Pion flash energy spectrum for $E_\pi=3$ GeV and associated muon backgrounds.

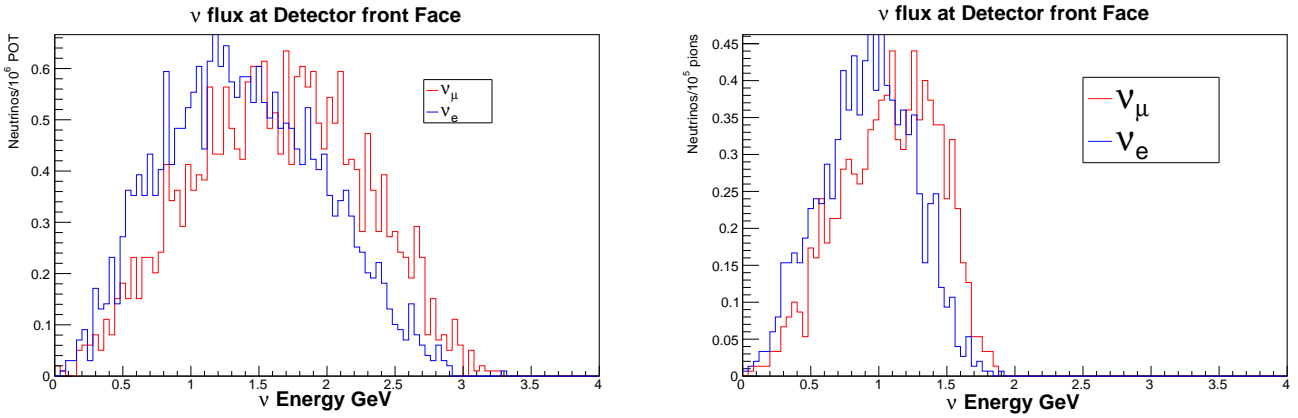


Figure 14: Signal neutrinos from muon decay. Left: ν_μ (Red) and ν_e (Blue) at $E_\pi=5$ GeV normalised to protons on target. Right: ν_μ (Red) and ν_e (Blue) at $E_\pi=3$ GeV normalised to pions entering the transfer line.

3.3.1 Pion flash neutrinos at $E_\pi=5$ GeV and 3 GeV

The biggest source of neutrinos are those from the pion flash. Figure 13 shows the energy spectrum of those pions. The plot on the left is for a central E_π of 5 GeV and right a central E_π of 3 GeV, in each case with a $\pm 10\%$ momentum bite, corresponding to the design parameters of the machine. The background from in-time muon decays is shown scaled up by a factor 40.

3.3.2 Muon signal neutrinos $E_\pi=5$ GeV and 3 GeV

The number of ν_μ 's and ν_e 's, which reach the front face of the detector is similar; their energy spectrum is similar with the ν_μ 's being slightly harder. We simulated three times as many events at 3 GeV in order to give us a comparable number of events at 3 GeV and 5 GeV. Dropping the central pion energy to 2 GeV loses another factor of 2. This energy dependence is largely due to the way the angular distribution of the neutrinos broadens as the Q value of the decay becomes a larger fraction of the beam's kinetic energy. The distance of the detector front face from the end of the production straight has not been optimised, but when we start detailed design of the hall and accelerator layout, it will be important to keep this distance as short as possible.

3.4 Event composition and kinematic distributions

Measurements of neutrino interaction cross-sections on various target nuclei has been a significant experimental focus in the last 10-15 years of neutrino physics as their importance to the systematics budget of the long baseline neutrino oscillation experiments became clear. In recent years the T2K experiment has produced data on ν_μ and ν_e interactions on scintillator at an average neutrino energy of 600 MeV[57–59], and the MINER ν A[32, 40, 60, 61] experiment has produced similar data but at average neutrino energies of 3 GeV and on a variety of target nuclei. The results of both experiments show that, although the primary lepton kinematics are reasonably well predicted by our models, the hadronic multiplicities, identities and kinematics are still poorly described. A detector for nuSTORM meeting the overarching requirements described above will address these issues.

In order to quantify the detector requirements, GENIE v3.06[62] was used to simulate neutrino interactions on a carbon nuclear target. As input to this simulation, the ν_μ flux for an initial pion energy of 5 GeV and 3 GeV discussed above were implemented. As the fluxes are not, presently, absolutely normalised, only the relative event category composition can be studied. The shapes of the kinematic distributions of final state particles which might be visible in a detector can, however, be used to inform the detector design.

The relative event rate composition for interactions of neutrinos from muon decay in the production straight is shown in table 2 for the 5 GeV and 3 GeV pion beams. For either pion energy, the event sample is dominated

ν_μ Channel	$E_\pi = 3$ GeV	$E_\pi = 5$ GeV
CC Quasi-elastic	0.41	0.32
2p2h	0.12	0.12
Resonance Production	0.43	0.49
Deep Inelastic	0.03	0.09
Coherent Pion	0.005	0.005

Table 2: Relative event category composition of ν_μ interactions in a Carbon target. Shown are the relative event rates using ν_μ from muon decay in the production straights, for two energies of initial pions from the target.

by the quasi-elastic and resonance interaction channels. The transition from quasi-elastic to resonant meson production is known as the dual region and is poorly understood. A large sample of neutrino interaction in this region would be crucial to understanding the physics. In addition, there is a smaller component of the Deep Inelastic Scattering (DIS) interaction channel. This is, however, in a low Q^2 and W^2 region, known as the Shallow Inelastic region. This region, which represents the transition from resonant meson production to the DIS region, is not well-understood, neither experimentally nor theoretically.

Figures 15, 16 and 17 show distributions from simulated muon neutrino interactions on carbon nuclei. The neutrinos were generated from muon decay in the production straight and are shown for initial pion energies of 5 GeV and 3 GeV. Figure 15 shows the energy of the primary muon and angle of the primary muon to the neutrino beam direction. The final state visible hadron multiplicity is shown in Figure 16, and the kinematics of protons produced in these interactions are shown in Figure 17.

4 Opportunity

nuSTORM will be the first neutrino-beam facility to be based on a stored muon beam and will provide a test-bed for the development of the technologies required for a multi-TeV Muon Collider and/or a Neutrino Factory. It will also serve the nuclear physics community by providing a unique probe of flavour-dependent

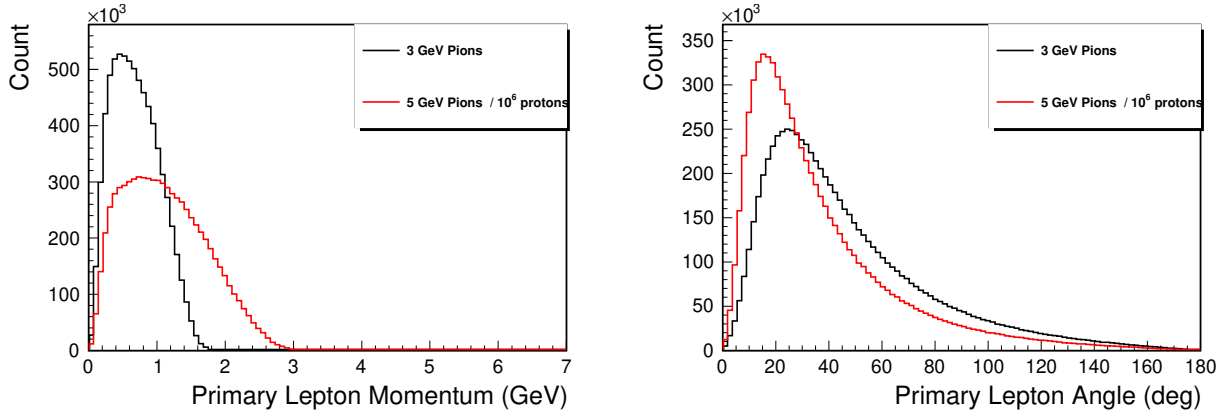


Figure 15: (Left) Momentum of the primary muon from ν_μ interactions on carbon. The neutrinos are generated from muon decay in the nuSTORM production straight and are generated with two different energies for the pions at the target. (Right) Angle of the primary muon from ν_μ interactions on carbon with respect to the beam direction.

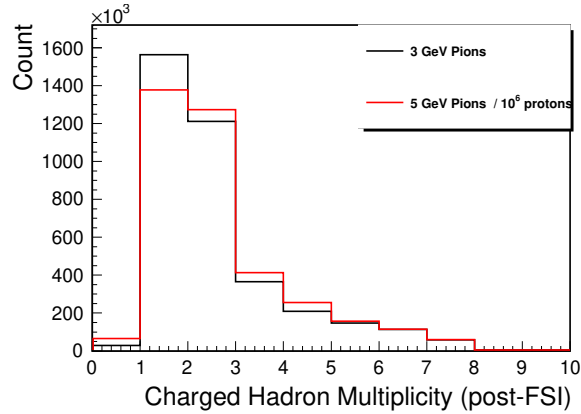


Figure 16: Charged hadron multiplicity in the detector.

collective effects in nuclei and a new tool to study the origin of nucleon spin. Both CERN and FNAL are ideally suited to the implementation of nuSTORM as the proton infrastructure at each laboratory is well-matched to the nuSTORM requirements and the scientific and technology-development outcomes of nuSTORM are an excellent match to both CERN's and FNAL's missions. It is conceivable that the implementation of nuSTORM will drive a step-change in capability comparable to that produced by Van der Meer's focusing horn and create a new technique for the study of the nature of matter and the forces that bind it.

The ENUBET [2–4] and nuSTORM [5, 6] collaborations have begun to work within and alongside the CERN Physics Beyond Colliders study group [7] and the international Muon Collider collaboration [8] to carry out a joint, five-year design study and R&D programme to deliver a concrete proposal for the implementation of an infrastructure in which:

- ENUBET and nuSTORM deliver the neutrino cross-section measurement programme identified in the recent update of the European Strategy for Particle Physics and allow sensitive searches for physics beyond the Standard Model to be carried out; and in which
- A 6D muon ionisation cooling experiment is delivered as part of the technology development programme defined by the international Muon Collider collaboration.

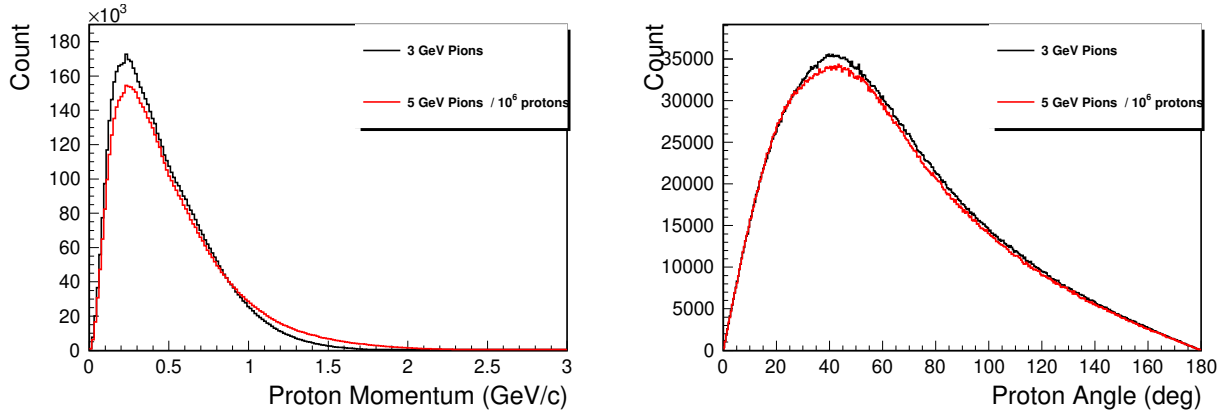


Figure 17: (Left) Momentum of protons in the hadronic final state of ν_μ interactions on carbon. The neutrinos are generated from muon decay in the nuSTORM production straight and are generated with two different energies for the pions at the target. (Right) Angle of protons in the hadronic final state from ν_μ interactions on carbon with respect to the beam direction.

This document summarises the status of the nuSTORM and 6D-cooling experiments and identifies opportunities for collaboration in the development of the initiative.

Strong synergies have been identified in the proton, target, meson-capture, and radiation-safety facility required to serve ENUBET (Enhanced NeUtrino BEams from kaon Tagging; NP06) [2–4], nuSTORM [5, 6], and the 6D muon ionisation cooling experiment. In the European context the study of a facility capable of serving ENUBET, nuSTORM and the 6D ionisation cooling demonstration experiment is mandated in the 2020 Update of the European Strategy for Particle Physics (ESPP) [1], which recommended that muon beam R&D should be considered a high-priority future initiative and that a programme of experimentation be developed to determine the neutrino cross-sections required to extract the most physics from the DUNE and Hyper-K long-baseline experiments. An initial concept for such a facility in which the target station is served by the PS proton beam is shown in figure 18 [45, 63].

The study of nuSTORM is now being taken forward in the context of the demonstrator facility required by the international Muon Collider collaboration that includes the 6D muon ionisation cooling experiment. The muon-beam development activity is being carried out in close partnership with the ENUBET collaboration and the Physics Beyond Colliders Study Group. The opportunity, therefore, is to forge an international collaboration to deliver on a five-year timescale a concrete proposal for the implementation of an infrastructure in which:

- ENUBET and nuSTORM deliver the neutrino cross-section measurement programme identified in the ESPP and allow sensitive searches for physics beyond the Standard Model to be carried out; and
- A 6D muon ionisation cooling experiment is delivered as part of the technology development programme defined by the international Muon Collider collaboration.

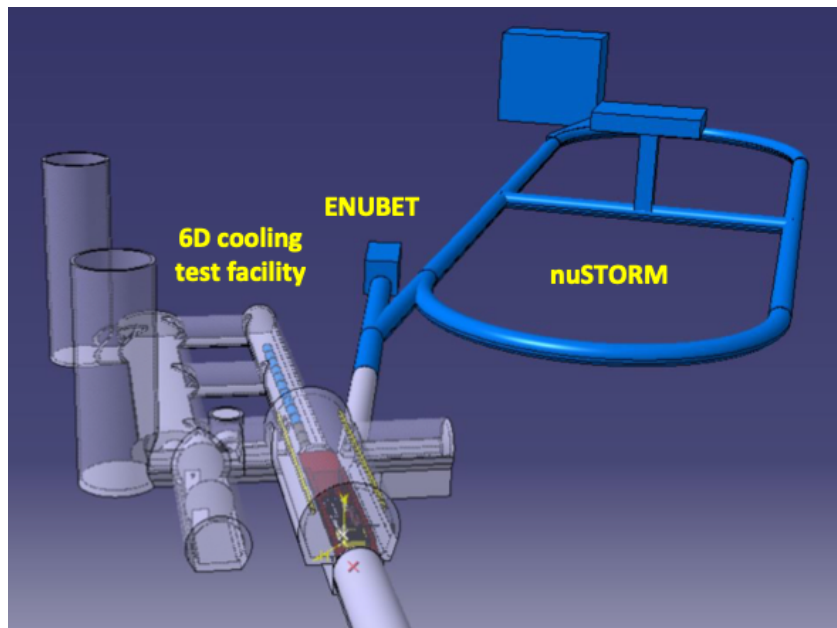


Figure 18: Schematic of a facility capable of serving ENUBET, nuSTORM and a 6D ionisation cooling facility on the CERN PS. The proton beam, entering from the bottom edge of the figure, impinges on the meson-production target placed in the neck of a horn which focuses accepted beam into a chicane in which the desired momentum bite is accepted. A magnetic switchyard and transfer lines then transport the resulting pion and kaon beams to the three experimental facilities [45, 63].

Appendix

A Simulation

The studies are based on preliminary simulations to estimate the fluxes of neutrinos which might be expected at the front face of a detector of volume 5 m x 5 m x 5 m placed 50 m downstream of the end of the nuSTORM production straight. This is purpose written code which tracks charged particles from the production target, down the transfer line into the production straight and for multiple turns round the nuSTORM ring. These particles are assumed to propagate down the optical axis of the machine and with uniform bending fields and without fringe fields. The pions decay with the correct distribution of lifetimes and produce muons and neutrinos with the correct kinematic distributions. The muons are likewise allowed to decay with the correct lifetime and the decay products are given the correct kinematic distributions. The resulting neutrinos are tracked and the position and momentum of those which cross the plane of the front face of the detector and are within 10 m of the detector centre are recorded. Those within ± 2.5 m in the vertical and horizontal plane are counted as the flux crossing the front face of the detector.

In order to improve the accuracy of the simulation, the distributions are smeared using the results of two other programmes. The momentum distribution and emittance of the pion beam which leaves the production region are modelled using FLUKA and these distributions define the starting conditions of the beam. The magnetic lattice of the transfer line and production straight are modelled using BDSIM. These numbers are used to model the emittance of the beam as it travels through the transfer line, down the production straight and is finally captured by the ring. The acceptance of the nuSTORM ring to muons is modelled using the results from [64]. This is used to smear the position and momentum of the decay products from both the pion decay and the subsequent muon decay.

B Background estimates

We have modelled the number of neutrinos we expect from the pion flash in the production straight and the background from muons which decay before they reach the first bend. We have also modelled the number of neutrinos produced by muons which are captured in the nuSTORM ring and subsequently decay. There are possible additional backgrounds to these two sources; we have investigated those and have ignored any background which is less than 1% of the signal. A summary of the calculations and reasoning is given below.

B.1 Decays in the transfer line at $E_\pi=5$ GeV

Neutrinos from pion decay in the transfer line which reach the detector will overlap in time from the decays in the production straight. Figure 19 shows the x and y distributions of neutrinos from pion decay in the transfer line at the plane of the detector front face. If we look at the y position (vertical) of the neutrinos which reach the plane, we see that the distribution is symmetrical and strongly peaked around zero. The x position has a similar shape, but the transfer line is at an angle to the production straight and so only the tail of the distribution passes through the detector front face. Only 11 neutrinos from 500k pions at the target arrive at the detector, compared with the pion flash in the production straight where 7138 neutrinos reach the detector from 50k pions; a contamination of less than 0.01%. The mean energy of these neutrinos is 0.06 GeV; in order to be thrown wide enough by the Q value from the decay to reach the detector, the neutrino must have a low energy in the nuSTORM rest frame. This source can therefore be ignored. Of the 81835 muons produced by pion decay 195 decay before the end of the transfer line and even if all the neutrinos produced by the muon decay reach the

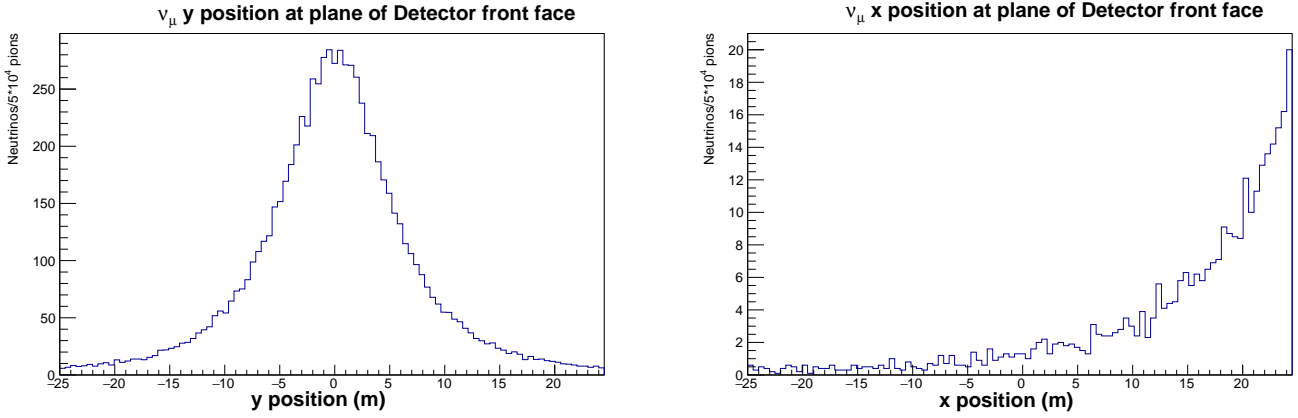


Figure 19: Neutrinos from pion decay in the transfer line at the plane defined by the front face of the detector. Y distribution (left), X distribution (right)

detector, then this represents only 0.27% of the flash signal. Although some of the muons will make it from the transfer line into the production straight, most of them will be absorbed by the material surrounding the beam tunnel, or by the material inside the tunnel. They will be brought to rest by about 15 m of soil. These muons will decay at rest and the resulting neutrinos will be distributed isotropically. The acceptance of a detector with a 25 m² front face at a distance of around 250 m means results in only 8 of these neutrinos being visible in the detector, and those at very low energy. We conclude that neutrinos from muon decay in the transfer line can also be ignored.

B.2 Decays in the transfer line at $E_{\pi}=3$ GeV

At 3 GeV the distribution is wider, as can be seen in Figure 20. The peak at zero is lower in the y position but the tail is higher in the x position. The combined effect of these is that 34 neutrinos arrive at the detector and their mean energy is slightly higher (0.10 GeV), because the forward beaming from the pion momentum is smaller and thus the Q value can push the resulting neutrinos out to wider angles. The contribution at less than 0.03% is still negligible. The muon decays in the production straight are still at a low level and even if the transfer line was directed straight at the detector they would still only produce a rate of around 0.2%.

The same argument on the muons which are brought to rest by the surrounding material, but in a shorter distance, applies for the 3 GeV sample.

Hence, decays in the transfer line for both pions and muons at pion energies of 3 and 5 GeV are at a level we ignore in this study.

B.3 Decays at the start of the first bend

We don't have a design which accurately models what happens to the pions as they enter the first bend at the end of the production straight. However we know from modelling of the transfer line that by the time the beam has been bent by 8 degrees neutrinos produced by the beam have only a small chance of reaching the detector. If we look at the number of pions which decay in the the arc as the beam turns through 8 degrees and assume that the acceptance for these neutrinos is the average of that for a beam at zero degrees and a beam at 8 degrees, then the background is about 1%. And since most pions will actually hit an absorber and at worst decay at rest, the actual background will be smaller and at much lower energies.

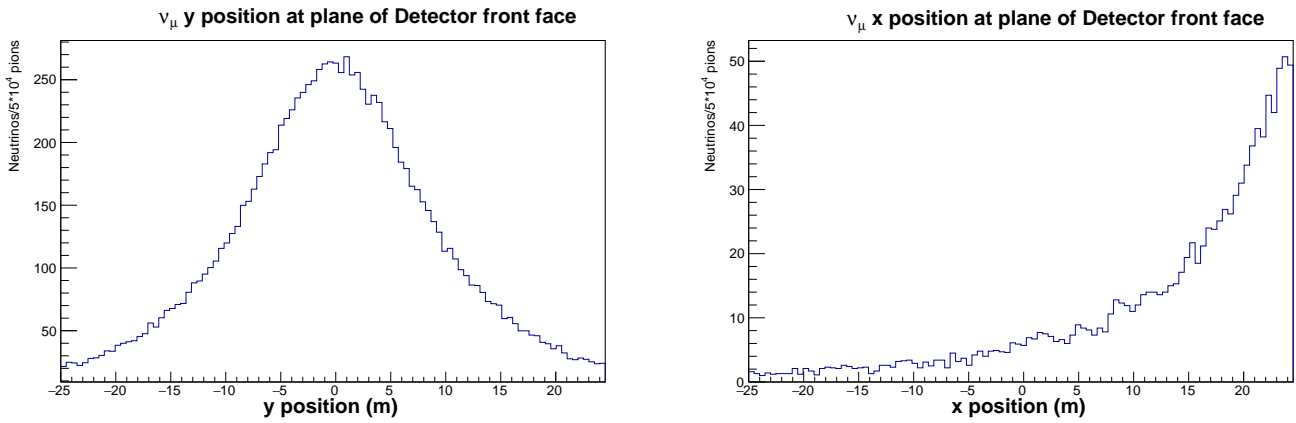


Figure 20: Neutrinos from pion decay in the transfer line at the plane defined by the front face of the detector. Y distribution (left), X distribution (right)

B.4 Kaons in the transfer line

We have not modelled Kaon kinematics, but the number produced at the target is significantly lower than the number of pions. Even if all of those decay, the number of Kaon decays is less than the number of pion decays and there is no reason to believe the acceptance for their neutrinos will be any greater than those from pion decays. We conclude the number of kaon neutrinos is much less than our 1% cutoff for modelling.

References

- [1] **European Strategy Group** Collaboration, *2020 Update of the European Strategy for Particle Physics*. CERN Council, Geneva, 2020.
- [2] ENUBET collaboration, “Enhanced NeUtrino BEams from kaon Tagging.” <https://www.pd.infn.it/eng/enubet/>. Accessed 08Mar22.
- [3] ENUBET collaboration, “Enhanced NeUtrino BEams from kaon Tagging.” <https://cordis.europa.eu/project/id/681647>. Accessed 08Mar22.
- [4] M. Torti *et al.*, “A high precision narrow-band neutrino beam: The ENUBET project,” *Int. J. Mod. Phys. A* **35** no. 34n35, (2020) 2044017.
- [5] nuSTORM collaboration, “nuSTORM, Neutrinos from Stored Muons.” <https://www.nustorm.org/trac/>. Accessed 08Mar22.
- [6] C. C. Ahdida *et al.*, “nuSTORM at CERN: Feasibility Study,” *CERN-PBC-REPORT-2019-003* (10, 2020) .
- [7] Physics Beyond Colliders study group, “The Physics Beyond Colliders Study Group.” <https://pbc.web.cern.ch>. Accessed 08Mar22.
- [8] Muon Collider collaboration, “Welcome to the Muon Collider Collaboration Website.” <https://muoncollider.web.cern.ch>. Accessed 08Mar22.
- [9] MICE collaboration, “International Muon Ionization Cooling Experiment.” <http://mice.iit.edu>. Accessed 08Mar22.
- [10] M. Bogomilov, R. Tsenov, G. Vankova-Kirilova, Y. P. Song, J. Y. Tang, Z. H. Li, R. Bertoni, M. Bonesini, F. Chignoli, R. Mazza, V. Palladino, A. de Bari, D. Orestano, L. Tortora, Y. Kuno, H. Sakamoto, A. Sato, S. Ishimoto, M. Chung, C. K. Sung, F. Filthaut, D. Jokovic, D. Maletic, M. Savic, N. Jovancevic, J. Nikolov, M. Vretenar, S. Ramberger, R. Asfandiyarov, A. Blondel, F. Drielsma, Y. Karadzhev, S. Boyd, J. R. Greis, T. Lord, C. Pidcott, I. Taylor, G. Charnley, N. Collomb, K. Dumbell, A. Gallagher, A. Grant, S. Griffiths, T. Hartnett, B. Martlew, A. Moss, A. Muir, I. Mullacrane, A. Oates, P. Owens, G. Stokes, P. Warburton, C. White, D. Adams, V. Bayliss, J. Boehm, T. W. Bradshaw, C. Brown, M. Courthold, J. Govans, M. Hills, J. B. Lagrange, C. Macwaters, A. Nichols, R. Preece, S. Ricciardi, C. Rogers, T. Stanley, J. Tarrant, M. Tucker, S. Watson, A. Wilson, R. Bayes, J. C. Nugent, F. J. P. Soler, G. T. Chatzitheodoridis, A. J. Dick, K. Ronald, C. G. Whyte, A. R. Young, R. Gamet, P. Cooke, V. J. Blackmore, D. Colling, A. Dobbs, P. Dornan, P. Franchini, C. Hunt, P. B. Jurj, A. Kurup, K. Long, J. Martyniak, S. Middleton, J. Pasternak, M. A. Uchida, J. H. Cobb, C. N. Booth, P. Hodgson, J. Langlands, E. Overton, V. Pec, P. J. Smith, S. Wilbur, M. Ellis, R. B. S. Gardener, P. Kyberd, J. J. Nebrensky, A. DeMello, S. Gourlay, A. Lambert, D. Li, T. Luo, S. Prestemon, S. Virostek, M. Palmer, H. Witte, D. Adey, A. D. Bross, D. Bowring, A. Liu, D. Neuffer, M. Popovic, P. Rubinov, B. Freemire, P. Hanlet, D. M. Kaplan, T. A. Mohayai, D. Rajaram, P. Snopok, Y. Torun, L. M. Cremaldi, D. A. Sanders, D. J. Summers, L. R. Coney, G. G. Hanson, C. Heidt, and M. collaboration, “Demonstration of cooling by the muon ionization cooling experiment,” *Nature* **578** no. 7793, (2020) 53–59. <https://doi.org/10.1038/s41586-020-1958-9>.

- [11] **ISS Physics Working Group** Collaboration, A. Bandyopadhyay *et al.*, “Physics at a future Neutrino Factory and super-beam facility,” *Rept. Prog. Phys.* **72** (2009) 106201, arXiv:0710.4947 [hep-ph].
- [12] **IDS-NF Collaboration** Collaboration, S. Choubey *et al.*, “International Design Study for the Neutrino Factory, Interim Design Report,” arXiv:1112.2853 [hep-ex].
- [13] J. C. Gallardo *et al.*, “Muon Collider: Feasibility Study,” 1996. <http://www.cap.bnl.gov/mumu/pubs/snowmass96/part6.pdf>. Prepared for 1996 DPF / DPB Summer Study on New Directions for High Energy Physics (Snowmass 96), Snowmass, Colorado, 25 Jun - 12 Jul 1996.
- [14] S. D. Holmes and V. D. Shiltsev, “Muon Collider,” arXiv:1202.3803 [physics.acc-ph].
- [15] **MAP Collaboration** Collaboration, D. M. Kaplan, “A Staged Muon-Based Neutrino and Collider Physics Program,” arXiv:1212.4214 [physics.acc-ph].
- [16] **NuSTEC** Collaboration, L. Alvarez-Ruso *et al.*, “NuSTEC White Paper: Status and challenges of neutrino–nucleus scattering,” *Prog. Part. Nucl. Phys.* **100** (2018) 1–68, arXiv:1706.03621 [hep-ph].
- [17] A. Branca, G. Brunetti, A. Longhin, M. Martini, F. Pupilli, and F. Terranova, “A New Generation of Neutrino Cross Section Experiments: Challenges and Opportunities,” *Symmetry* **13** no. 9, (2021) 1625, arXiv:2108.12212 [hep-ex].
- [18] H. Duyang, B. Guo, S. R. Mishra, and R. Petti, “A Precise Determination of (Anti)neutrino Fluxes with (Anti)neutrino-Hydrogen Interactions,” *Phys. Lett. B* **795** (2019) 424–431, arXiv:1902.09480 [hep-ph].
- [19] X.-G. Lu, D. Coplowe, R. Shah, G. Barr, D. Wark, and A. Weber, “Reconstruction of Energy Spectra of Neutrino Beams Independent of Nuclear Effects,” *Phys. Rev. D* **92** no. 5, (2015) 051302, arXiv:1507.00967 [hep-ex].
- [20] P. Hamacher-Baumann, X.-G. Lu, and J. Martín-Albo, “Neutrino-hydrogen interactions with a high-pressure time projection chamber,” *Phys. Rev. D* **102** no. 3, (2020) 033005, arXiv:2005.05252 [physics.ins-det].
- [21] A. S. Meyer, A. Walker-Loud, and C. Wilkinson, “Status of Lattice QCD Determination of Nucleon Form Factors and their Relevance for the Few-GeV Neutrino Program,” arXiv:2201.01839 [hep-lat].
- [22] S. X. Nakamura *et al.*, “Towards a Unified Model of Neutrino-Nucleus Reactions for Neutrino Oscillation Experiments,” *Rept. Prog. Phys.* **80** no. 5, (2017) 056301, arXiv:1610.01464 [nucl-th].
- [23] M. Sajjad Athar and J. G. Morfín, “Neutrino(antineutrino)–nucleus interactions in the shallow- and deep-inelastic scattering regions,” *J. Phys. G* **48** no. 3, (2021) 034001, arXiv:2006.08603 [hep-ph].
- [24] V. Pandey, N. Jachowicz, M. Martini, R. González-Jiménez, J. Ryckebusch, T. Van Cuyck, and N. Van Dessel, “Impact of low-energy nuclear excitations on neutrino-nucleus scattering at MiniBooNE and T2K kinematics,” *Phys. Rev. C* **94** no. 5, (2016) 054609, arXiv:1607.01216 [nucl-th].

- [25] **DUNE** Collaboration, R. Acciarri *et al.*, “Long-Baseline Neutrino Facility (LBNF) and Deep Underground Neutrino Experiment (DUNE): Conceptual Design Report, Volume 2: The Physics Program for DUNE at LBNF,” arXiv:1512.06148 [physics.ins-det].
- [26] C. Wilkinson *et al.*, “Testing charged current quasi-elastic and multinucleon interaction models in the NEUT neutrino interaction generator with published datasets from the MiniBooNE and MINERvA experiments,” *Phys. Rev. D* **93** no. 7, (2016) 072010, arXiv:1601.05592 [hep-ex].
- [27] **T2K** Collaboration, K. Abe *et al.*, “Measurement of double-differential muon neutrino charged-current interactions on C₈H₈ without pions in the final state using the T2K off-axis beam,” *Phys. Rev. D* **93** no. 11, (2016) 112012, arXiv:1602.03652 [hep-ex].
- [28] M. B. Barbaro, A. De Pace, and L. Fiume, “The SuSA Model for Neutrino Oscillation Experiments: From Quasielastic Scattering to the Resonance Region,” *Universe* **7** no. 5, (2021) 140, arXiv:2104.10472 [hep-ph].
- [29] **MINERvA** Collaboration, P. A. Rodrigues *et al.*, “Identification of nuclear effects in neutrino-carbon interactions at low three-momentum transfer,” *Phys. Rev. Lett.* **116** (2016) 071802, arXiv:1511.05944 [hep-ex]. [Addendum: *Phys.Rev.Lett.* 121, 209902 (2018)].
- [30] **NOvA, R. Group** Collaboration, M. A. Acero *et al.*, “Adjusting neutrino interaction models and evaluating uncertainties using NOvA near detector data,” *Eur. Phys. J. C* **80** no. 12, (2020) 1119, arXiv:2006.08727 [hep-ex].
- [31] U. Mosel, “Neutrino event generators: foundation, status and future,” *J. Phys. G* **46** no. 11, (2019) 113001, arXiv:1904.11506 [hep-ex].
- [32] **MINERvA** Collaboration, X.-G. Lu *et al.*, “Exploring neutrino–nucleus interactions in the GeV regime using MINERvA,” *Eur. Phys. J. ST* **230** no. 24, (2021) 4243–4257, arXiv:2107.02064 [hep-ex].
- [33] X.-G. Lu, L. Pickering, S. Dolan, G. Barr, D. Coplowe, Y. Uchida, D. Wark, M. O. Wascko, A. Weber, and T. Yuan, “Measurement of nuclear effects in neutrino interactions with minimal dependence on neutrino energy,” *Phys. Rev. C* **94** no. 1, (2016) 015503, arXiv:1512.05748 [nucl-th].
- [34] A. P. Furmanski and J. T. Sobczyk, “Neutrino energy reconstruction from one muon and one proton events,” *Phys. Rev. C* **95** no. 6, (2017) 065501, arXiv:1609.03530 [hep-ex].
- [35] X.-G. Lu and J. T. Sobczyk, “Identification of nuclear effects in neutrino and antineutrino interactions on nuclei using generalized final-state correlations,” *Phys. Rev. C* **99** no. 5, (2019) 055504, arXiv:1901.06411 [hep-ph].
- [36] T. Golan, C. Juszczak, and J. T. Sobczyk, “Final State Interactions Effects in Neutrino-Nucleus Interactions,” *Phys. Rev. C* **86** (2012) 015505, arXiv:1202.4197 [nucl-th].
- [37] T. Leitner, L. Alvarez-Ruso, and U. Mosel, “Charged current neutrino nucleus interactions at intermediate energies,” *Phys. Rev. C* **73** (2006) 065502, arXiv:nucl-th/0601103.
- [38] T. Leitner, O. Buss, L. Alvarez-Ruso, and U. Mosel, “Electron- and neutrino-nucleus scattering from the quasielastic to the resonance region,” *Phys. Rev. C* **79** (2009) 034601, arXiv:0812.0587 [nucl-th].

- [39] O. Buss, T. Gaitanos, K. Gallmeister, H. van Hees, M. Kaskulov, O. Lalakulich, A. B. Larionov, T. Leitner, J. Weil, and U. Mosel, “Transport-theoretical Description of Nuclear Reactions,” *Phys. Rept.* **512** (2012) 1–124, arXiv:1106.1344 [hep-ph].
- [40] **MINERvA** Collaboration, D. Coploue *et al.*, “Probing nuclear effects with neutrino-induced charged-current neutral pion production,” *Phys. Rev. D* **102** no. 7, (2020) 072007, arXiv:2002.05812 [hep-ex].
- [41] W. Altmannshofer, S. Gori, M. Pospelov, and I. Yavin, “Neutrino Trident Production: A Powerful Probe of New Physics with Neutrino Beams,” *Phys. Rev. Lett.* **113** (2014) 091801, arXiv:1406.2332 [hep-ph].
- [42] L. Alvarez-Ruso and E. Saul-Sala, “Neutrino interactions with matter and the MiniBooNE anomaly,” *Eur. Phys. J. ST* **230** no. 24, (2021) 4373–4389, arXiv:2111.02504 [hep-ph].
- [43] W. Abdallah, R. Gandhi, and S. Roy, “Requirements on common solutions to the LSND and MiniBooNE excesses: a post-MicroBooNE study,” arXiv:2202.09373 [hep-ph].
- [44] **nuSTORM** Collaboration, D. Adey *et al.*, “Light sterile neutrino sensitivity at the nuSTORM facility,” *Phys. Rev. D* **89** no. 7, (2014) 071301, arXiv:1402.5250 [hep-ex].
- [45] C. Adolphsen *et al.*, “European Strategy for Particle Physics - Accelerator R&D Roadmap,” arXiv:2201.07895 [physics.acc-ph].
- [46] D. Stratakis and R. B. Palmer, “Rectilinear six-dimensional ionization cooling channel for a muon collider: A theoretical and numerical study,” *Phys. Rev. ST Accel. Beams* **18** (Mar, 2015) 031003. <https://link.aps.org/doi/10.1103/PhysRevSTAB.18.031003>.
- [47] N. V. Mokhov and C. C. James, “The MARS Code System User’s Guide Version 15(2016),”.
- [48] T.T. Böhlen, F. Cerutti, M.P.W. Chin, A. Fassò, A. Ferrari, P.G. Ortega, A. Mairani, P.R. Sala, G. Smirnov and V. Vlachoudis, “*The FLUKA Code: Developments and Challenges for High Energy and Medical Applications*,” Tech. Rep. Nuclear Data Sheets 120, 211-214 (2014), 2014.
- [49] A. Fasso, A. Ferrari, J. Ranft, and P. R. Sala, “Fluka: a multi-particle transport code,” Tech. Rep. CERN-2005-10 and SLAC-R-773, 2005.
- [50] L. Nevay *et al.*, “Recent BDSIM Related Developments and Modeling of Accelerators,” *JACoW IPAC2021* (2021) THPAB214.
- [51] **nuSTORM** Collaboration, D. Adey *et al.*, “nuSTORM - Neutrinos from STORed Muons: Proposal to the Fermilab PAC,” arXiv:1308.6822 [physics.acc-ph].
- [52] A. Liu, A. Bross, and D. Neuffer, “A FODO racetrack ring for nuSTORM: design and optimization,” *JINST* **12** no. 07, (2017) P07018, arXiv:1704.00798 [physics.acc-ph].
- [53] J.-B. Lagrange, R. Appleby, J. Garland, J. Pasternak, and S. Tygier, “Racetrack FFAg muon decay ring for nuSTORM with triplet focusing,” *Journal of Instrumentation* **13** no. 09, (Sep, 2018) P09013–P09013. <https://doi.org/10.1088%2F1748-0221%2F13%2F09%2Fp09013>.
- [54] A. Blanchet, “Physics and Performance of the Upgraded T2K’s Near Detector,” *Phys. At. Nucl.* **84** no. 4, (2021) 519–523.

- [55] **DUNE** Collaboration, A. Abed Abud *et al.*, “Deep Underground Neutrino Experiment (DUNE) Near Detector Conceptual Design Report,” *Instruments* **5** no. 4, (2021) 31, arXiv:2103.13910 [physics.ins-det].
- [56] A. Bersani, A. D. Bross, B. Caiffi, L. Di Noto, P. Fabbriatore, S. Farinon, F. Ferraro, D. V. Mitchell, R. Musenich, and M. Pallavicini, “A Solenoid With Partial Yoke for the Dune Near Detector,” *IEEE Trans. Appl. Supercond.* **31** no. 5, (2021) 4500404.
- [57] **T2K** Collaboration, K. Abe *et al.*, “Measurements of $\bar{\nu}_\mu$ and $\bar{\nu}_\mu + \nu_\mu$ charged-current cross-sections without detected pions or protons on water and hydrocarbon at a mean anti-neutrino energy of 0.86 GeV,” *PTEP* **2021** no. 4, (2021) 043C01, arXiv:2004.13989 [hep-ex].
- [58] **T2K** Collaboration, K. Abe *et al.*, “Simultaneous measurement of the muon neutrino charged-current cross section on oxygen and carbon without pions in the final state at T2K,” *Phys. Rev. D* **101** no. 11, (2020) 112004, arXiv:2004.05434 [hep-ex].
- [59] **T2K** Collaboration, S. Jenkins, “T2K latest results on neutrino-nucleus cross sections,” *J. Phys. Conf. Ser.* **2156** (2021) 012151.
- [60] **MINERvA** Collaboration, T. Cai *et al.*, “Nucleon binding energy and transverse momentum imbalance in neutrino-nucleus reactions,” *Phys. Rev. D* **101** no. 9, (2020) 092001, arXiv:1910.08658 [hep-ex].
- [61] **MINERvA** Collaboration, X.-G. Lu *et al.*, “Measurement of final-state correlations in neutrino muon-proton mesonless production on hydrocarbon at $\langle E_\nu \rangle = 3$ GeV,” *Phys. Rev. Lett.* **121** no. 2, (2018) 022504, arXiv:1805.05486 [hep-ex].
- [62] C. Andreopoulos *et al.*, “The GENIE Neutrino Monte Carlo Generator,” *Nucl. Instrum. Meth. A* **614** (2010) 87–104, arXiv:0905.2517 [hep-ph].
- [63] F. S. Esteban, M. Calviani, D. Calzolari, R. F. Ximenes, A. Krainer, A. Lechner, R. Losito, C. Rogers, and D. Schulte, “Muon Collider Graphite Target Studies and Demonstrator Layout Possibilities at CERN,” *Proc. 13th International Particle Accelerator Conference (IPAC’22)* no. 13, (07, 2022) 2895–2898. <https://jacow.org/ipac2022/papers/thpotk052.pdf>.
- [64] J.-B. Lagrange, R. Appleby, J. Garland, J. Pasternak, and S. Tygier, “Racetrack FFAG muon decay ring for nuSTORM with triplet focusing,” *JINST* **13** no. 9, (2018) P09013, arXiv:1806.02172 [physics.acc-ph].

The nuSTORM collaboration

Canada

S. Bhadra, S. Menary

Department of Physics and Astronomy, York University, 4700 Keele Street, Toronto, Ontario, M3J 1P3, Canada

M. Hartz[†]

TRIUMF, 4004 Wesbrook Mall, Vancouver, BC V6T 2A3, Canada

[†] *Also at Kavli Institute for the Physics and Mathematics of the Universe, The University of Tokyo Kashiwa Campus, 5-1-5 Kashiwanoha, Kashiwa, Chiba 277-8583, Japan*

China

J. Tang

Institute of High Energy Physics, Chinese Academy of Sciences, Beijing, China

Germany

U. Mosel

Justus Liebig Universität, Ludwigstraße 23, 35390 Gießen, Germany

M.V. Garzelli

II. Institut für Theoretische Physik, Universität Hamburg, Luruper Chaussee 149, 22761 Hamburg, Germany

W. Winter

Deutsches Elektronen-Synchrotron (DESY), Platanenallee 6, 15738 Zeuthen, Germany

India

S. Goswami, K. Chakraborty

Physical Research Laboratory, Ahmedabad 380009, India

S.K. Agarwalla

Institute of Physics, Sachivalaya Marg, Sainik School Post, Bhubaneswar 751005, Orissa, India

Italy

E. Santopinto

INFN Sezione di Genova, Via Dodecaneso, 33-16146, Genova, Italy

M. Bonesini

Sezione INFN Milano Bicocca, Dipartimento di Fisica G. Occhialini, Milano, Italy

L. Stanco

INFN, Sezione di Padova, 35131 Padova, Italy

D. Orestano, L. Tortora

INFN Sezione di Roma Tre and Dipartimento di Matematica e Fisica, Università Roma Tre, Roma, Italy

Japan

Y. Mori

Kyoto University Institute for Integrated Radiation and Nuclear Science (KURNS), 2, Asashiro-Nishi, Kumatori-cho, Sennan-gun, Osaka 590-0494, Japan

Y. Kuno, A. Sato

Osaka University, Graduate School, School of Science, 1-1 Machikaneyama-cho, Toyonaka, Osaka 560-0043, Japan

South Korea

M. Chung

UNIST, Ulsan, Korea

The Netherlands

F. Filthaut[†]

Nikhef, Amsterdam, The Netherlands

[†] *Also at Radboud University, Nijmegen, The Netherlands*

Poland

J.T. Sobczyk

Institute of Theoretical Physics, University of Wrocław, pl. M. Borna 9,50-204, Wrocław, Poland

Spain

J.J. Gomez-Cadenas

Donostia International Physics Center (DIPC), Paseo Manuel de Lardizabal 4, 20018 Donostia-San Sebastián, Gipuzkoa, Spain

J.A. Hernando Morata

Universidade de Santiago de Compostela (USC), Departamento de Física de Partículas, E-15706 Santiago de Compostela, Spain

L. Alvarez Ruso, A. Cervera, A. Donini, P. Hernandez, J. Lopez Pavon[†], J. Martín-Albo, O. Mena, P. Novella, M. Sorel

Instituto de Física Corpuscular (IFIC), Centro Mixto CSIC-UVEG, Edificio Institutos Investigación, Paterna, Apartado 22085, 46071 Valencia, Spain

[†] *Theoretical Physics Department, CERN, 1211 Geneva 23, Switzerland*

Sweden

R. Ruber

Department of Physics and Astronomy, Uppsala University, Ångströmlaboratoriet, Lägerhyddsvägen 1, Box 516, 751 20 Uppsala, Sweden

Switzerland

C.C. Ahdida, W. Bartmann, J. Bauche, M. Calviani, N. Charitonidis, J. Gall, B. Goddard, C. Hessler, J. Kopp[†],
M. Lamont, J.A. Osborne, E. Radicioni, A. de Roeck, F.M. Velotti
CERN, CH-1211, Geneva 23, Switzerland

[†] Also at *PRISMA Cluster of Excellence, Johannes Gutenberg University, Mainz, Germany*

A. Blondel, E.N. Messomo, F. Sanchez Nieto
University de Geneve, 24, Quai Ernest-Ansermet, 1211 Geneva 4, Suisse

United Kingdom

M.A. Uchida
Cavendish Laboratory (HEP), JJ Thomson Avenue, Cambridge, CB3 0HE, UK

S. Easo, R.E. Edgecock, J.B. Lagrange, W. Murray, C. Rogers
STFC Rutherford Appleton Laboratory, Chilton, Didcot, Oxfordshire, OX11 0QX, UK

J.J. Back, G. Barker, S.B. Boyd, P.F. Harrison
Department of Physics, University of Warwick, Coventry, CV4 7AL, UK

S. Pascoli
Institute for Particle Physics Phenomenology, Department of Physics, University of Durham, Science Laboratories, South Rd, Durham, DH1 3LE, UK

S.-P. Hallsjö, F.J.P. Soler
School of Physics and Astronomy, Kelvin Building, University of Glasgow, Glasgow G12 8QQ, Scotland, UK

H.M. O’Keeffe, L. Kormos, J. Nowak, P. Ratoff
Physics Department, Lancaster University, Lancaster, LA1 4YB, UK

C. Andreopoulos[†], N. McCauley, C. Touramanis
Department of Physics, Oliver Lodge Laboratory, University of Liverpool, Liverpool, L69 7ZE, UK
[†] Also at *STFC, Rutherford Appleton Laboratory, Harwell Campus, Chilton, Didcot, OX11 0QX, UK*

T. Alves, D. Colling, P. Dornan, P. Dunne, P. Franchini, P.M. Jonsson, P.B. Jurj, A. Kurup, P. Litchfield,
K. Long[†], T. Nonnenmacher, M. Pfaff*, J. Pasternak[†], M. Scott, J.K. Sedgbeer, W. Shorrocks, M.O. Wascko
Physics Department, Blackett Laboratory, Imperial College London, Exhibition Road, London, SW7 2AZ, UK
[†] Also at *STFC, Rutherford Appleton Laboratory, Harwell Campus, Chilton, Didcot, OX11 0QX, UK*
* Also at *Technical University of Munich (TUM), Arcisstrasse 21 D-80333 Munich, Germany*

F. di Lodovico, T. Katori
King’s College London, Strand, London WC2R 2LS, UK

A. Bevan, L. Cremonesi, P. Hobson
Queen Mary University of London, Mile End Road, London E1 4NS, UK

R. Nichol

Department of Physics and Astronomy, University College London, Gower Street, London, WC1E 6BT, UK

R. Appleby, S. Tygier

The University of Manchester, 7.09, Schuster Laboratory, Manchester, M13 9PL, UK and the Cockcroft Institute, Daresbury Laboratory, WA4 4AD, UK

X. Lu, D. Wark, A. Weber[†]

Particle Physics Department, The Denys Wilkinson Building, Keble Road, Oxford, OX1 3RH, UK

[†] *Also at STFC, Rutherford Appleton Laboratory, Harwell Campus, Chilton, Didcot, OX11 0QX, UK*

P.J. Smith

University of Sheffield, Dept. of Physics and Astronomy, Hicks Bldg., Sheffield S3 7RH, UK

P. Kyberd, D.R. Smith

College of Engineering, Design and Physical Sciences, Brunel University London, Uxbridge, Middlesex, UB8 3PH, UK

United States of America

S.J. Brice, A.D. Bross, S. Chattopadhyay[†], S. Feher, L. Fields, P. Hanlet, N. Mokhov, J.G. Morfín, D. Neuffer, J. Paley, S. Parke, Z. Pavlovic, M. Popovic, P. Rubinov, V. Shiltzev

Fermilab, P.O. Box 500, Batavia, IL 60510-5011, USA

[†] *Northern Illinois University, 1425 W. Lincoln Hwy., DeKalb, IL 60115-2828, USA*

P. Huber, C. Mariani, J.M. Link

Virginia Polytechnic Inst. and State Univ., Physics Dept., Blacksburg, VA 24061-0435

B. Freemire, A. Liu

Euclid Techlabs, LLC, 365 Remington Blvd, Bolingbrook, IL, 60440, USA

D.M. Kaplan, P. Snopok

Illinois Institute of Technology, Chicago, IL, USA

S.R. Mishra

Department of Physics and Astronomy, University of South Carolina, Columbia SC 29208, USA

K. Mahn

High Energy Physics, Biomedical-Physical Sciences Bldg., Michigan State University, 220 Trowbridge Rd, East Lansing, MI 48824, USA

A. de Gouvêa

Northwestern University, Dept. of Physics and Astronomy, 2145 Sheridan Road, Evanston, Illinois 60208-3112 USA

V. Pandey

Department of Physics, University of Florida, Gainesville, FL 32611, USA

Y. Onel, D. Winn

Department of Physics and Astronomy, The University of Iowa, 203 Van Allen Hall, Iowa City, Iowa 52242-1479, USA

H.A. Tanaka

SLAC National Accelerator Laboratory, 2575 Sand Hill Rd, Menlo Park, CA 94025, USA

M. Hostert

School of Physics and Astronomy, University of Minnesota, Minneapolis, MN 55455, USA

S.A. Bogacz

Thomas Jefferson National Accelerator Facility, 12000 Jefferson Avenue, Newport News, VA 23606, USA

L. Cremaldi, D. Summers

University of Mississippi, Oxford, MS, USA

K.T. McDonald

Princeton University, Princeton, NJ, 08544, USA

G. Hanson

Department of Physics and Astronomy, University of California, Riverside, CA 92521, US

M. Palmer

Brookhaven National Laboratory, P.O. Box 5000, Upton, NY 11973 USA

M. Liu

Purdue University, 610 Purdue Mall, West Lafayette, IN, 47907, 765-494-4600, USA